LAMINAR BOUNDARY LAYERS ON BODIES OF REVOLUTION: COMPUTER PROGRAMS AND VORTICITY BUDGETS

By R. E. Sheridan, Jr.

Technical Memorandum
File No. TM 502.2421-19
July 26, 1968
Contract NOw 65-0123-d
Copy No. 11

The Pennsylvania State University
Institute for Science and Engineering
ORDNANCE RESEARCH LABORATORY
University Park, Pennsylvania

NAVY DEPARTMENT · NAVAL ORDNANCE SYSTEMS COMMAND

Abstract: The incompressible laminar boundary layer equations are solved for flow about a sphere and an ellipsoid using a finite difference scheme. The effects of vortex stretching on the momentum and vorticity equations are studied.

TABLE OF CONTENTS

Page

ACKNOWLEDGMENTS ii

LIST OF FIGURES iv

LIST OF TABLES v

LIST OF SYMBOLS vi

INTRODUCTION 1

DEVELOPMENT OF EQUATIONS 4

Boundary Layer Equations 4

Displacement Thickness and Skin Friction 10

Vorticity Relationships 11

METHOD OF SOLUTION 15

Basic Scheme 15

Solution in the x-Direction 15

Solution of the Ordinary Differential Equation 19

Integration Procedure 21

RESULTS AND CONCLUSIONS 26

Discussion of Results 26

Conclusions 42

APPENDIX A: COMPUTER PROGRAM FOR SOLVING THE BOUNDARY LAYER EQUATIONS 44

APPENDIX B: CALCULATION OF M AND R FOR AN ELLIPSOID 55

REFERENCES 60

LIST OF FIGURES

Figure		Page
1	Coordinate System	5
2	Coordinate and Notation System	17
3	Typical Integration Trials	23
4	f''_w for a Sphere	27
5	δ_1^* for a Sphere	28
6	f''_w for an Ellipsoid	29
7	δ_1^* for an Ellipsoid	30
8	Dimensionless Terms of the Vorticity Equation for a Sphere	33
9	Dimensionless Terms of the Vorticity Equation for a Sphere	34
10	Dimensionless Terms of the Vorticity Equation for a Sphere	35
11	Dimensionless Terms of the Vorticity Equation for a Sphere	36
12	Dimensionless Terms of the Vorticity Equation for an Ellipsoid	37
13	Dimensionless Terms of the Vorticity Equation for an Ellipsoid	38
14	Dimensionless Terms of the Vorticity Equation for an Ellipsoid	39
15	Dimensionless Terms of the Vorticity Equation for an Ellipsoid	40

LIST OF TABLES

Table		Page
1	COMPARISON OF VALUES OF f''_w ON A SPHERE AS CALCULATED BY THE PRESENT METHOD AND THE METHOD DUE TO SMITH AND CLUTTER	31

LIST OF SYMBOLS

a	Semi-major axis of an ellipsoid
a_1, a_2, a_3	Numerical correction parameters
b	Semi-minor axis of an ellipsoid
c_f	Local skin friction coefficient
e	Eccentricity of an ellipsoid
f	Dimensionless stream function
h	Step length in η
h_x, h_y, h_θ	Metric coefficients
K	Longitudinal curvature
M	Pressure gradient parameter
r_o	Radius of a body of revolution
R	Radius-change parameter for a body of revolution
u	x-component of velocity within the boundary layer
U	x-component of velocity outside the boundary layer
U_∞	Free stream velocity
v	y-component of velocity within the boundary layer
w	θ-component of velocity within the boundary layer
x	Distance along the surface from the leading edge
X	Distance measured along the axis of a body from the leading edge
y	Distance normal to the surface

δ	Boundary layer thickness
δ_1^*	Dimensionless displacement thickness
ϵ	A constant used as a numerical bound to values of ϕ'
η	Dimensionless distance normal to the surface
η_∞	A point representing $\eta = \infty$, which in computation is located slightly beyond the "edge" of the boundary layer
θ	An orthogonal coordinate (see Figure 1)
μ	Dimensionless axial distance for an ellipsoid
ν	Kinematic viscosity
ϕ	A transformed stream function (dimensionless)
ψ	Stream function
ω_θ	θ-component of vorticity

CHAPTER I

INTRODUCTION

The primary purpose of this study is to develop a rapid and accurate method for solving the incompressible laminar boundary layer equations for axisymmetric flow using a digital computer. In order to obtain some qualitative insight into the trends exhibited by model calculations, the effects of vortex stretching on the momentum and vorticity equations are studied.

There are many methods available for obtaining solutions to the boundary layer equations; a fact easily verified by consulting a standard reference such as Meksyn (1961), Rosenhead (1963) or Schlichting (1960). The majority of these techniques can be classified as follows: (1) momentum integral methods, (2) correlation methods, (3) infinite series method and (4) finite difference procedures. In general, the first two techniques are approximate procedures in the sense that the original equations have been compromised. The infinite series and finite difference methods, on the other hand, are considered to be theoretically exact in the limit, that is, for an infinite number of terms and vanishingly small step lengths, respectively. Since it is impossible to discuss all of the individual techniques in each category, only a few representative examples are discussed below.

The Pohlhausen[12] and Thwaites[14] methods are well-known examples of the integral and correlation techniques. In the first of these, a polynomial expansion for the velocity is assumed and then the momentum integral equation is solved. Thwaites' procedure is based on an empirical correlation of existing exact and approximate flow solutions. Using this known data, Thwaites tabulated various boundary layer shape parameters from which approximate values for the momentum and displacement thicknesses can be readily determined.

The method described by Frossling[12] is typical of the infinite series type of solution. Here, the body contour and the potential flow are expressed as power series in x (distance measured along the body). The stream function is also expanded in an infinite series in x with coefficients depending on the wal' distance y. These series are then substituted into the boundary layer equations, written in terms of the stream function and, consequently, an N^{th} order set of ordinary differential equations results for the unknown coefficients.

Finally, the Hartree-Womersley[5] scheme is considered as an illustration of the finite difference type. Briefly, this technique utilizes a simple transformation of the momentum equation in which x, y remain essentially as independent variables. The region of the boundary layer is divided into vertical strips and the transformed momentum equation is solved numerically at each step.

The method chosen for this paper is based on a finite difference procedure developed by A. M. O. Smith and Darwin W. Clutter[13] which is actually an extension of the Hartree-Womersley scheme. The most important reasons for its selection are (1) it is more accurate for a wider variety of problems than the approximate integral or correlation techniques, (2) there is considerably less computational work involved compared to the infinite series approach when high accuracy is required, (3) it exhibits a greater degree of numerical stability than other finite difference methods, and (4) the equations on which this procedure is based are free of singularities. In the adaptation of Smith's and Clutter's method, the "starting" procedure (see Reference 13 and Page 20 of this study) for the integration of the boundary layer equations and the process for obtaining the final solutions for the shear stress and velocity profiles at each location along the body were revised.

In the sections that follow, the necessary equations and the method for their solution are developed. The relevant computer program presented in Appendix A was executed for a sphere and an ellipsoid, and the results are discussed in Chapter IV.

CHAPTER II

DEVELOPMENT OF EQUATIONS

Boundary Layer Equations

The equations to be solved cover the case of axisymmetric, steady flow past a blunt-nosed body of revolution. The curvilinear coordinates of a point P in space are taken as (x, y, θ). The basic notation and scheme of coordinates is shown in Figure 1; U_∞ is the free stream velocity, and $U(x)$ is the velocity in the x-direction just outside the boundary layer. Theta (θ) is the angle between a fixed meridian plane and the meridian plane containing P. The surfaces Γ_1 = constant and Γ_2 = constant are taken as surfaces of revolution about the axis OX, and are such that, if C is the curve of intersection of the surface of the body by a meridan plane, then the sections of the surfaces Γ_1 = constant and Γ_2 = constant are normals to C and parallel curves to C, respectively. Consequently, Γ_1 may be taken as the distance x from the forward stagnation point O measured along C, and Γ_2 as the normal distance y from the surface. Here u, v, and w are the components of velocity in the directions of increasing x, y, and θ, respectively; and r_o, the body radius, is the distance from P_c to OX, so that r_o is a function of x alone. The coordinates

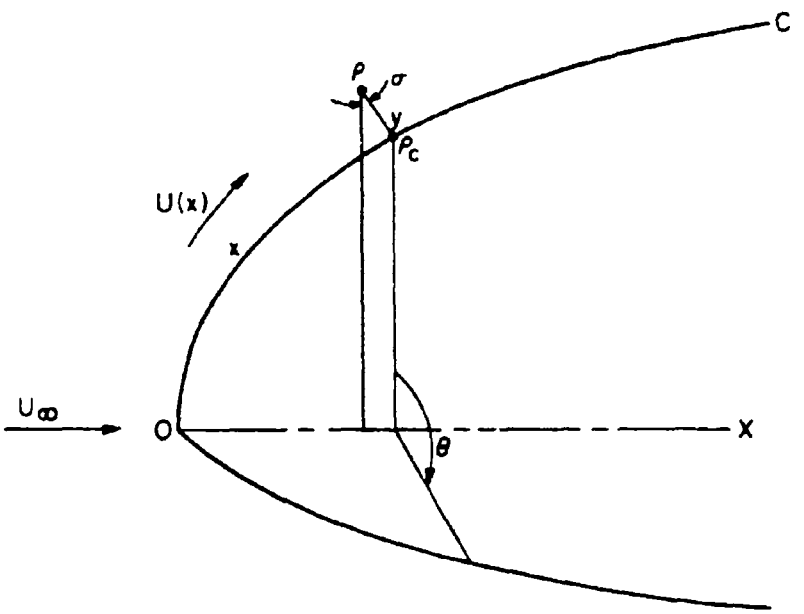

Figure 1 Coordinate System

(x, y, θ) form a mutually orthogonal system with the following metric coefficients:

$$h_x = 1 + Ky,$$

$$h_y = 1,$$

and

$$h_\theta = r = r_o + y \cos \sigma,$$

where K (a function of x) is the longitudinal curvature and r is the radial distance from P to OX[11].

For flows at high Reynolds numbers, around bodies whose local radius r_o is large compared to the boundary layer thickness δ (that is, $\delta/r_o \ll 1$) and whose surface contains no large variations in longitudinal curvature (e.g., sharp corners where d^2r_o/dx^2 becomes infinite) so that $dK/dx \sim 1$, the product $K\delta$ is small[9]. Hence, the above metric coefficients can now be approximated by:

$$h_x = 1,$$

$$h_y = 1, \qquad (1)$$

and

$$h_\theta = r_o,$$

where the domain of y is restricted to the boundary layer[4, 10]. Since the motion is independent of θ and $w = 0$, the boundary layer equations are:[4, 8, 10, 12]

$$u \frac{\partial u}{\partial x} + v \frac{\partial u}{\partial y} = U \frac{dU}{dx} + \nu \frac{\partial^2 u}{\partial y^2} \quad \text{(Momentum)}, \tag{2}$$

and

$$\frac{\partial (u r_o)}{\partial x} + \frac{\partial (v r_o)}{\partial y} = 0 \quad \text{(Continuity)}. \tag{3}$$

The boundary conditions are, with the subscript w denoting wall conditions:

$$\begin{aligned} y = 0 &: u_w = 0 \\ &\quad v_w = 0 \\ y \to \infty &: u \to U(x). \end{aligned} \tag{4}$$

Equations (2) and (3) can be combined into a single equation through the introduction of the stream function ψ[10]. Let

$$u = \frac{1}{r_o} \frac{\partial}{\partial y} (\psi r_o) = \frac{\partial \psi}{\partial y}$$

and

$$v = - \frac{1}{r_o} \frac{\partial}{\partial x} (\psi r_o) = - \frac{\partial \psi}{\partial x} - \frac{\psi}{r_o} \frac{dr_o}{dx}.$$

The resulting equation is:

$$\frac{\partial \psi}{\partial y} \frac{\partial^2 \psi}{\partial x \partial y} - \left(\frac{\partial \psi}{\partial x} + \frac{\psi}{r_o} \frac{dr_o}{dx} \right) \frac{\partial^2 \psi}{\partial y^2} = U \frac{dU}{dx} + \nu \frac{\partial^3 \psi}{\partial y^3}, \tag{5}$$

with the boundary conditions:

$$y = 0 : \left(\frac{\partial \psi}{\partial y} \right)_w = 0, \; \psi_w = 0,$$

and

$$y \longrightarrow \infty : \frac{\partial \psi}{\partial y} \longrightarrow U(x). \tag{6}$$

A more convenient representation of Equation (5) is obtained through the use of a transformation first introduced by Falkner and Skan[4]. In their transformation, a dimensionless height η and a dimensionless stream function f are introduced:

$$\eta = \left(\frac{U}{\nu x}\right)^{\frac{1}{2}} y, \quad \psi = (U\nu x)^{\frac{1}{2}} f(x, \eta). \tag{7}$$

If the relations (7) are substituted into Equation (5), and if $\partial f/\partial \eta$ is represented by f', etc., then the following equation results:

$$f''' = -\left(\frac{M+1}{2} + R\right) ff'' + M(f'^2 - 1) + x\left[f' \frac{\partial f'}{\partial x} - f'' \frac{\partial f}{\partial x}\right]. \tag{8}$$

The term $R = \frac{x}{r_o} \frac{dr_o}{dx}$ is a measure of local increases in body radius, $M = \frac{x}{U} \frac{dU}{dx}$ is a pressure gradient parameter, and $f' = \frac{u}{U}$. The boundary conditions for Equation (8) are:

$$\eta = 0 : f'_w = 0, \; f_w = 0$$

and (9)

$$\eta \longrightarrow \infty : f' \longrightarrow 1.$$

For computational purposes, it is necessary to obtain the third derivative of f evaluated at the wall. From Equation (8) and the application of the conditions (9), it can be shown that

$$f'''_w = -M. \tag{10}$$

Considering Equation (8), when R = 0 and M is constant, the bracketed expression containing the partial derivatives with respect to x vanishes and the following ordinary non-linear differential equation is obtained[4]:

$$f''' = -\left(\frac{M+1}{2}\right) ff'' + M(f'^2 - 1).$$

This relationship provides a family of "similar" solutions.

A final transformation is applied to Equation (8) for the purpose of numerical calculations. The quantity ϕ is introduced, such that:

$$f = \phi + \eta,$$

$$f' = \phi' + 1, \tag{11}$$

and

$$f'' = \phi'', \text{ etc.}$$

Equation (8) becomes:

$$\phi''' = -\left(\frac{M+1}{2} + R\right)(\phi+\eta)\ \phi'' + M(\phi'^2 + 2\phi') + x\left[(\phi' +1)\ \frac{\partial \phi'}{\partial x} - \phi''\ \frac{\partial \phi}{\partial x}\right], \tag{12}$$

with the boundary conditions:

$$\eta = 0 : \phi_w = 0,\ \phi'_w = -1$$

and $$\eta \longrightarrow \infty : \phi' \longrightarrow 0. \tag{13}$$

Equation (12) has several noteworthy advantages over other possible representations: one is the fact that the starting process is very simple. At $x = 0$, all x-dependence is removed, leaving only an ordinary differential equation to solve. A second advantage of Equation (12) is that almost all of the variation in boundary layer thickness has been eliminated. The thickness in the transformed system seldom varies by more than 50 percent over a range of x, whereas the actual physical boundary layer thickness might vary by a factor of 10 or higher. Finally, it is very important to note that these equations are entirely free of mathematical "pathologies." They are well behaved at $x = 0$, and solutions of Equation (12) exhibit an asymptotic convergence nature for large η[2, 13].

Displacement Thickness and Skin Friction

The displacement thickness δ_1 is given by[12]:

$$\delta_1 = \int_0^\infty \left(1 - \frac{u}{U}\right) dy.$$

In nondimensional form, this becomes:

$$\delta_1^* = \frac{\delta_1}{x}\sqrt{\frac{Ux}{\nu}} = \int_0^\infty (1-f') \, d\eta.$$

After utilizing Equations (9) and (11), the nondimensional displacement thickness becomes:

$$\delta_1^* = \lim_{\eta \to \infty} (\eta - f) = - \phi_\infty . \tag{14}$$

The local skin friction coefficient C_f is defined as the ratio of the local shear stress τ at the wall to the local dynamic pressure outside the boundary layer. The relation is:

$$C_f = \frac{\mu \left(\frac{du}{dy}\right)_w}{\frac{1}{2}\rho U^2} = 2 \left(\frac{\nu}{Ux}\right)^{\frac{1}{2}} f''_w = 2 \left(\frac{\nu}{Ux}\right)^{\frac{1}{2}} \phi''_w , \tag{15}$$

where

$$\left(\frac{du}{dy}\right)_w = \left(\frac{U^3}{\nu x}\right)^{\frac{1}{2}} f''_w = \left(\frac{U^3}{\nu x}\right)^{\frac{1}{2}} \phi''_w .$$

The parameters δ_1^* and f''_w are very useful in studying the growth of the boundary layer and the variation in skin friction along a body's surface. Graphs and some additional discussion of these quantities for a spherical and an ellipsoidal body are presented in Chapter IV.

Vorticity Relationships

The coordinate system illustrated in Figure 1, the assumptions made on Pages 4 and 6, and the metric coefficients Equation (1) are used here to develop the vorticity equation. It is assumed that v is negligibly small, and the magnitude of the gradients in the y-direction is much greater than the x-wise gradients. Also, since w = 0 and the θ-wise gradients are zero

for axisymmetric flow, then it is a relatively simple task to show that the only significant vorticity component is the θ component ω_θ[4]. The relation for ω_θ, consistent with the approximations made above, is:

$$\omega_\theta = - \frac{\partial u}{\partial y} . \tag{16}$$

The momentum Equation (2) is differentiated with respect to y and rearranged to give:

$$u \frac{\partial}{\partial x}\left(\frac{\partial u}{\partial y}\right) + v \frac{\partial}{\partial y}\left(\frac{\partial u}{\partial y}\right) = - \frac{\partial u}{\partial y}\left(\frac{\partial u}{\partial x} + \frac{\partial v}{\partial y}\right) + \nu \frac{\partial^2}{\partial y^2}\left(\frac{\partial u}{\partial y}\right). \tag{17}$$

Now, the indicated differentiations in the continuity Equation (3) are carried out, yielding the expression

$$\frac{\partial u}{\partial x} + \frac{\partial v}{\partial y} = - \frac{u}{r_o} \frac{dr_o}{dx} . \tag{18}$$

Finally, Equations (16) and (18) are substituted into Equation (17) to obtain the vorticity transport equation:

$$u \frac{\partial \omega_\theta}{\partial x} + \frac{\partial \omega_\theta}{\partial y} = \frac{\omega_\theta u}{r_o} \frac{dr_o}{dx} + \nu \frac{\partial^2 \omega_\theta}{\partial y^2} . \tag{19}$$

The terms on the left-hand side of this relation are the familiar convection terms. The last term is recognized as the rate of change due to molecular diffusion of vorticity. The first quantity on the right-hand side of Equation (19) is a vortex stretching effect.

If this term is rewritten as:

$$\frac{\omega_\theta u}{2\pi r_o} \frac{d\,(2\pi r_o)}{dx},$$

then it clearly represents a change in vorticity due to the extension or contraction of vortex-lines resulting from the variation in body circumference with x. There is an intensification of vorticity due to the extension of vortex-lines when $d(2\pi r_o)/dx$ is positive[1]. Consequently, the vortex stretching term is a source of vorticity for bodies whose radius increases downstream.

In order to study the terms of Equation (19), it is again convenient to introduce the stream function ψ for u and v and the transformation defined by Equation (7). The nondimensionalized terms of the vorticity transport equation become

$$\frac{u\,\dfrac{\partial \omega_\theta}{\partial x}}{\dfrac{U^2}{x}\left(\dfrac{U}{\nu x}\right)^{\frac{1}{2}}} = -\left[x\,\frac{\partial f''}{\partial x} + \tfrac{1}{2}\,(3M-1)\,f''\right] f' \quad \text{(u-convection)},$$

$$\frac{v\,\dfrac{\partial \omega_\theta}{\partial y}}{\dfrac{U^2}{x}\left(\dfrac{U}{\nu x}\right)^{\frac{1}{2}}} = \left[x\,\frac{\partial f}{\partial x} + \tfrac{1}{2}\,(1+M+2R)\,f\right] f''' \quad \text{(v-convection)},$$

$$\frac{\dfrac{\omega_\theta u}{r_o}\dfrac{dr_o}{dx}}{\dfrac{U^2}{x}\left(\dfrac{U}{\nu x}\right)^{\frac{1}{2}}} = -\,Rf'f'' \quad \text{(stretching)},$$

and

$$\frac{\nu \dfrac{\partial^2 \omega_\theta}{\partial y^2}}{\dfrac{U^2}{x}\left(\dfrac{U}{\nu x}\right)^{\frac{1}{2}}} = -f^{iv} \qquad \text{(diffusion)}. \tag{20}$$

Each term of Equation (19) can now be computed from the solutions obtained for Equation (12).

CHAPTER III

METHOD OF SOLUTION

Basic Scheme

The method of solution that is used in this work is based on a method developed by Smith and Clutter[13]. They replaced the x-wise partial derivatives in Equation (12) by finite difference approximations as originally suggested by Hartree and Womersley (1937). The equation is converted to an ordinary differential equation. If the flow in the x-direction is divided into n stations, then the ordinary differential equation has to be solved n times in succession, since M and R as well as ϕ, ϕ', and ϕ'' vary with x. The numerical methods used are a form of the ordinary finite difference treatment since discrete variable approximations are made in both the x and η directions.

Solution in the x-Direction

Two finite difference representations of Equation (12) are possible. The first is called the "point" form. Here, the differential equation is written to apply at a point; that is, the x-derivatives at a point are replaced by their finite difference equivalents. The second treatment is to deal in terms of mean values of the variable ϕ over a finite region; this is referred to as the "mean" form.

After extensive calculations, using both the "point" and "mean" forms, Smith and Clutter found that the "point" forms were generally more accurate and exhibited a greater degree of stability. In particular, the "point" form with three and four points proved to be the most accurate of all[13].

The basic scheme of the finite difference representation is illustrated in Figure 2. The variables M and R are known as functions of x. The lines x_n, x_{n-1}, x_{n-2}, etc., partition the x, η space into a number of regions. Since Equation (12) is parabolic in form, it must be solved in the direction of increasing x. It is assumed that the solution $\phi(\eta)$ and its derivatives ϕ' and $\phi''(\eta)$ are known at all stations up to and including x_{n-1}. The problem is to obtain the solution at x_n. To accomplish this, the "point" method is applied to Equation (12) at x_n.

The two, three, and four-point "point" forms that replace the x-wise partial derivatives in Equation (12) are easily obtained by differentiating the Lagrangian interpolating polynomials of two, three, and four points, respectively. In the actual computer program, these formulas are written to handle unequal step lengths. For the sake of simplicity only, the four-point formula for equal step length is presented here.

The four-point formulas for $\left(\frac{\partial \phi}{\partial x}\right)_n$ and $\left(\frac{\partial \phi'}{\partial x}\right)_n$ including the error terms are:

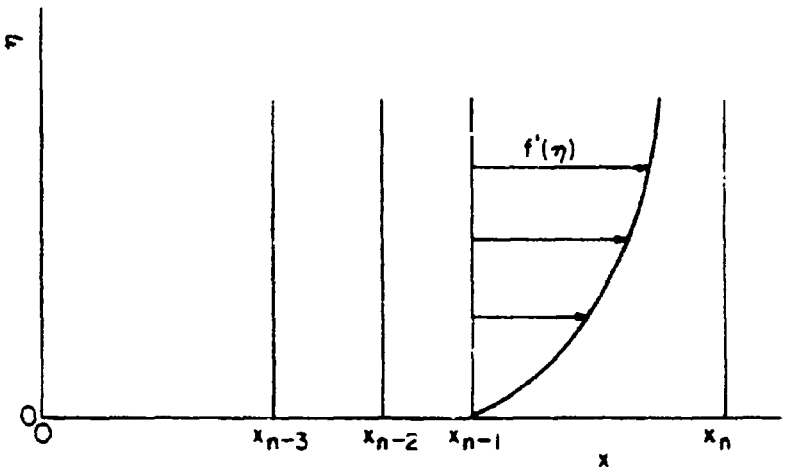

Figure 2 Coordinate and Notation System

$$\left(\frac{\partial \phi}{\partial x}\right)_n = \frac{11\phi_n - 18\phi_{n-1} + 9\phi_{n-2} - 2\phi_{n-3}}{6\Delta x} + \frac{(\Delta x)^3}{4}\frac{\partial^4 \phi(\xi)}{\partial x^4} , \qquad (21)$$

and

$$\left(\frac{\partial \phi'}{\partial x}\right)_n = \frac{11\phi'_n - 18\phi'_{n-1} + 9\phi'_{n-2} - 2\phi'_{n-3}}{6\Delta x} + \frac{(\Delta x)^3}{4}\frac{\partial^4 \phi'(\xi)}{\partial x^4} , \qquad (22)$$

where $x_{n-3} \leq \xi(x) \leq x_n^3$. The error terms indicate that these relationships are of third-order accuracy and become exact for third-degree polynomial variations.

If Equations (21) and (22), without the error terms, are substituted into Equation (12), the following equation for the four-point approximation results:

$$\phi'''_n = -\left(\frac{M_n + 1}{2} + R_n\right)(\phi_n + \eta)\,\phi''_n + M_n\,(\phi'^2_n + 2\phi'_n) + \frac{x_n}{6\Delta x_n}\Big[(\phi'_n + 1)\,(11\phi'_n - 18\phi'_{n-1} + 9\phi'_{n-2} - 2\phi'_{n-3}) - \phi''_n\,(11\phi_n - 18\phi_{n-1} + 9\phi_{n-2} - 2\phi_{n-3})\Big]. \qquad (23)$$

Consequently, Equation (12) has been transformed into an ordinary non-linear differential equation at x_n.

It is important to observe that the ratic $x/\Delta x$, rather than the step length Δx, is a primary parameter. In fact, Smith and Clutter found that this ratio should not exceed 25 for a stable solution using single-precision arithmetic on a digital computer.

Solution of the Ordinary Differential Equation

The ordinary differential Equation (23) is solved with a predictor-corrector (or extrapolation-interpolation) technique. The formulas used in this method are developed in Collatz' book[2]. The four-point predictor relationships written in Lagrangian form, including the local error terms, are:

$$\phi_{i+1} = \phi_i + h\phi_i' + \frac{h^2}{2}\phi_i'' + \frac{h^3}{720}\left[188\phi_i''' - 123\phi_{i-1}''' + 72\phi_{i-2}''' - 17\phi_{i-3}'''\right] + 0(h^7), \tag{24}$$

$$\phi_{i+1}' = \phi_i' + h\phi_i'' + \frac{h^2}{360}\left[323\phi_i''' - 264\phi_{i-1}''' + 159\phi_{i-2}''' - 38\phi_{i-3}'''\right] + 0(h^6), \tag{25}$$

and

$$\phi_{i+1}'' = \phi_i'' + \frac{h}{24}\left[55\phi_i''' - 59\phi_{i-1}''' + 37\phi_{i-2}''' - 9\phi_{i-3}'''\right] + 0(h^5). \tag{26}$$

The corresponding corrector type equations are:

$$\phi_{i+1} = \phi_i + h\phi_i' + \frac{h^2}{2}\phi_i'' + \frac{h^3}{720}\left[17\phi_{i+1}''' + 120\phi_i''' - 21\phi_{i-1}''' + 4\phi_{i-2}'''\right] - 0(h^7), \tag{27}$$

$$\phi_{i+1}' = \phi_i' + h\phi_i'' + \frac{h^2}{360}\left[36\phi_{i+1}''' + 171\phi_i''' - 36\phi_{i-1}''' + 7\phi_{i-2}'''\right] - 0(h^6), \tag{28}$$

and

$$\phi_{i+1}'' = \phi_i'' + \frac{h}{24}\left[9\phi_{i+1}''' + 19\phi_i''' - 5\phi_{i-1}''' + \phi_{i-2}'''\right] - 0(h^5). \tag{29}$$

In these formulas, h is the step length in the η-direction and i is the step count. The procedure is to make a prediction by means of Equations (24), (25), and (26). Using these values in Equation (23), ϕ'''_{i+1} is computed; then, Equations (27), (28), and (29) are employed to obtain improved results. As a consequence of the fact that the above relationships provide a high degree of accuracy, this single improvement is sufficient for each η step.

The solution is started at the first point by a Maclaurin expansion which is used as a predictor. The series for ϕ has the form:

$$\phi_p = \phi_w + h\phi'_w + \frac{h^2}{2}\phi''_w + \frac{h^3}{6}\phi'''_w \quad , \tag{30}$$

and similarly for ϕ'_p and ϕ''_p. The values of ϕ_p, ϕ'_p and ϕ''_p are substituted into Equation (23) to find the extrapolated quantity ϕ'''_p. These extrapolated values are used to compute improved values by Obrechkoff's corrector type formula (Hildebrand, 1956):

$$\phi_c = \phi_w + \frac{h}{2}(\phi'_p + \phi'_w) - \frac{h^2}{10}(\phi''_p - \phi''_w) + \frac{h^3}{120}(\phi'''_p + \phi'''_w) - O(h^7), \tag{31}$$

with corresponding relations for ϕ'_c and ϕ''_c. An improved value for ϕ''' is now computed from Equation (23). The improved quantities ϕ_c, ϕ'_c and ϕ''_c are now substituted for the predicted results ϕ_p, ϕ'_p and ϕ''_p into equations of the type (31) to produce further improved values. This iterative process is repeated several times until the convergence of ϕ'''_c is effected. This method of integration

is now extended to the next two points by using two- and three-point formulas of the same family as the four-point relations presented above. Finally, the four-point formulas can be utilized.

A constant η-step length h is used except for the first four points where its values is h/4. The same η-step sizes are used throughout the entire x-range since most of the variation in boundary layer thickness has been removed (cf. Page 10).

Integration Procedure

In general, a non-linear boundary value problem with two-point boundary conditions, one point being an asymptotic condition at $\eta = \infty$, can be rather difficult to solve. However, in this case, a simple method consists of solving it as an initial value problem using an arbitrary value of the unknown condition ϕ''_w at the initial point. It is then necessary to search among the single infinity of possible values of the unknown condition for the particular value which allows the boundary conditions to be satisfied asymptotically at the second point.

The essence of the present method is to seek in a systematic manner the value of ϕ''_w such that Equation (23) is satisfied in conjunction with

$$\phi = 0,\ \phi' = -1 \text{ at } \eta = 0,$$

and

$$|\phi'| \leq \varepsilon \text{ at } \eta = \eta_\infty.$$

where ε is a prescribed small quantity. The detailed process, illustrated in Figure 3, is as follows:

1) Choose an initial estimate for ϕ''_w and a value for η_∞.
2) Solve Equation (23) by "marching" outward away from the wall using the technique outlined in the preceding section.
3) Continue until
   (a) $\phi' > -\varepsilon$, or
   (b) $\eta = \eta_\infty$.
4) If 3(b) occurs before 3(a), then the initial estimate for ϕ''_w was too low. Therefore, ϕ''_w is increased by an appropriate amount a_1 and the process is started over again at step 2. This case is indicated by curve (a) in Figure 3.
5) If 3(a) occurs, then there are three possibilities:
   (a) $|\phi'| < \varepsilon$ and $\eta = \eta_\infty$. When this occurs, an acceptable solution for ϕ''_w has been found. This situation is represented by curve (b) in Figure 3.
   (b) $\phi' > \varepsilon$ (high trial). This indicates that the initial estimate of ϕ''_w was high. It is reduced by a small amount a_2 and the process is repeated again from step 2. See curve (c) in Figure 3.

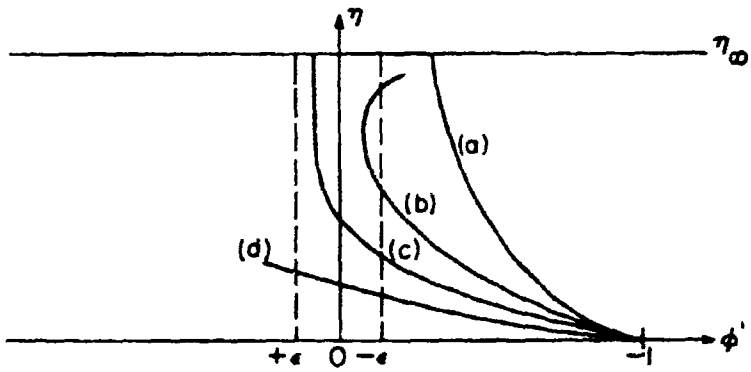

Figure 3 Typical Integration Trials

(c) $\phi' < \varepsilon$. Continue "marching" until either 5(a) or 5(b) occurs or ϕ' becomes less than $-\varepsilon$. If $\phi' < -\varepsilon$ (low trial), then the initial value for ϕ''_w was low and a new estimate is found by adding a small increment a_3 and then the procedure is started over again at step 2 (curve (d) in Figure 3).

6) When a high and a low trial are found, a new value for ϕ''_w is obtained from the arithmetic mean of these trials. This averaging will lead to convergence because ϕ'_∞ varies almost linearly with ϕ''_w for a wide variety of flow problems investigated by Smith and Clutter.

7) After step 6 has been executed, the estimates for ϕ''_w are continually improved by taking the mean of the best high and low pairs.

8) When three values of ϕ''_w are obtained that satisfy the condition that $|\phi'| < \varepsilon$ and $\eta = \eta_\infty$, then the final solution is found by forming a simple three-point interpolation.

9) Proceed to the next x-station and use the final value of ϕ''_w from step 8 of the previous station as the initial guess for ϕ''_w.

It should be mentioned that this method is not completely devoid of difficulties. As the integration proceeds downstream in the x-direction, a great sensitivity to initial estimates of ϕ''_w develops. In fact, it becomes virtually impossible to find any solution where ϕ' is kept within the range $\pm \varepsilon$. This problem is most probably a result of the following causes: (1) the value of η_∞ and the associated asymptotic boundary condition; (2) the value of ε; (3) the accumulative error due to the product of the four-point-interpolation errors with the ratio $x/\Delta x$; (4) round-off error; (5) a coupling effect of all or some of these factors.

After a considerable number of trial calculations, it was found that this difficulty can be effectively overcome by lowering η_∞ and increasing ε by small increments. However, these changes in either η_∞ or ε should be kept as small as possible in order to minimize the attendant error in the final value of ϕ''_w.

CHAPTER IV

RESULTS AND CONCLUSIONS

Discussion of Results

A computer program was written to solve the equation of motion (12) with the associated boundary conditions (13). The program was executed for the cases of a sphere and an ellipsoid with an eccentricity of 1/2 (semi-major axis a = 2 and semi-minor axis b = 1.73205) in a meridian plane. The nondimensional displacement thickness δ_1^* and f_w'' [see Equation (16)] for both bodies of revolution are illustrated in Figures 4 through 7. In Table I, a comparison between the present method and that due to Smith and Clutter is given for the sphere.

In these graphs, the curves denoted by R = 0 represent the special case when r_o is constant. The increase in boundary layer displacement thickness is a consequence of the fact that the vorticity generated on the body's surface is transported chiefly due to the action of viscous diffusion, while the effect of convection towards the wall is negligible. Whereas, in flows where r_o varies, there are the opposing actions of convection toward the wall and viscous diffusion away from it. Consequently, the boundary layer grows more rapidly and the skin friction (shear stress at the wall) is smaller in magnitude for the case when r_o is constant compared to the case when r_o varies.

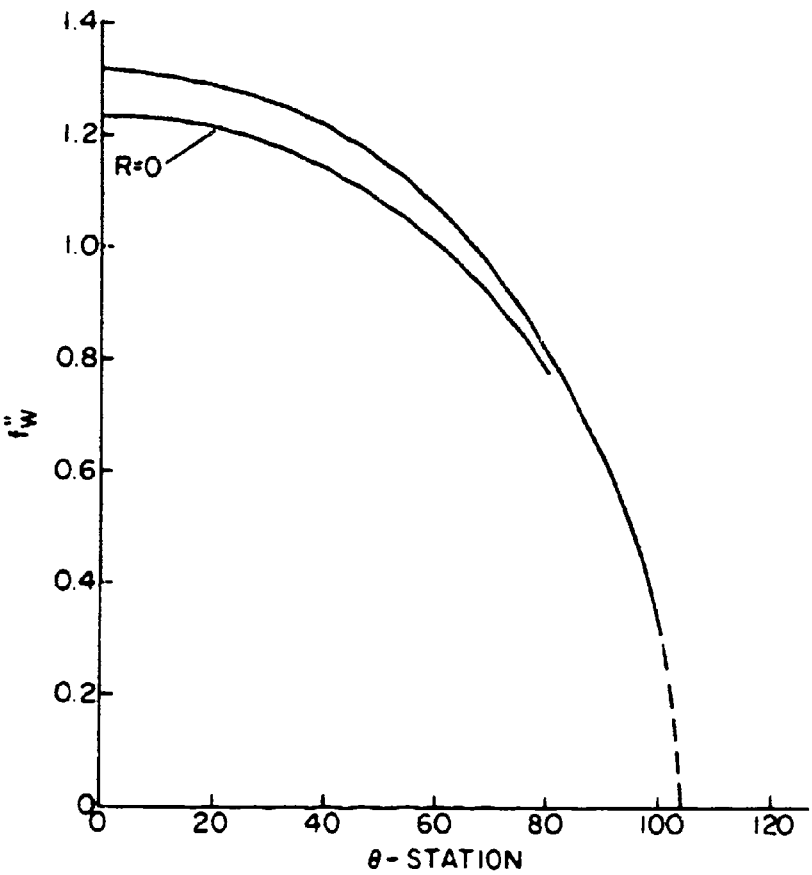

Figure 4 f''_w for a Sphere

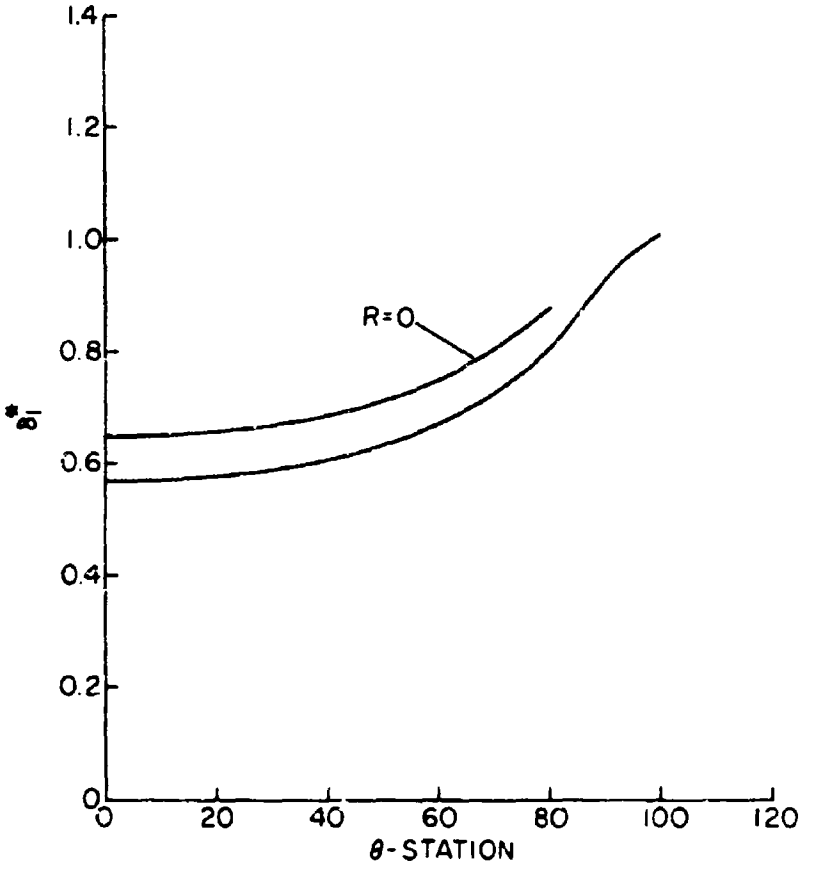

Figure 5 δ_1^* for a Sphere

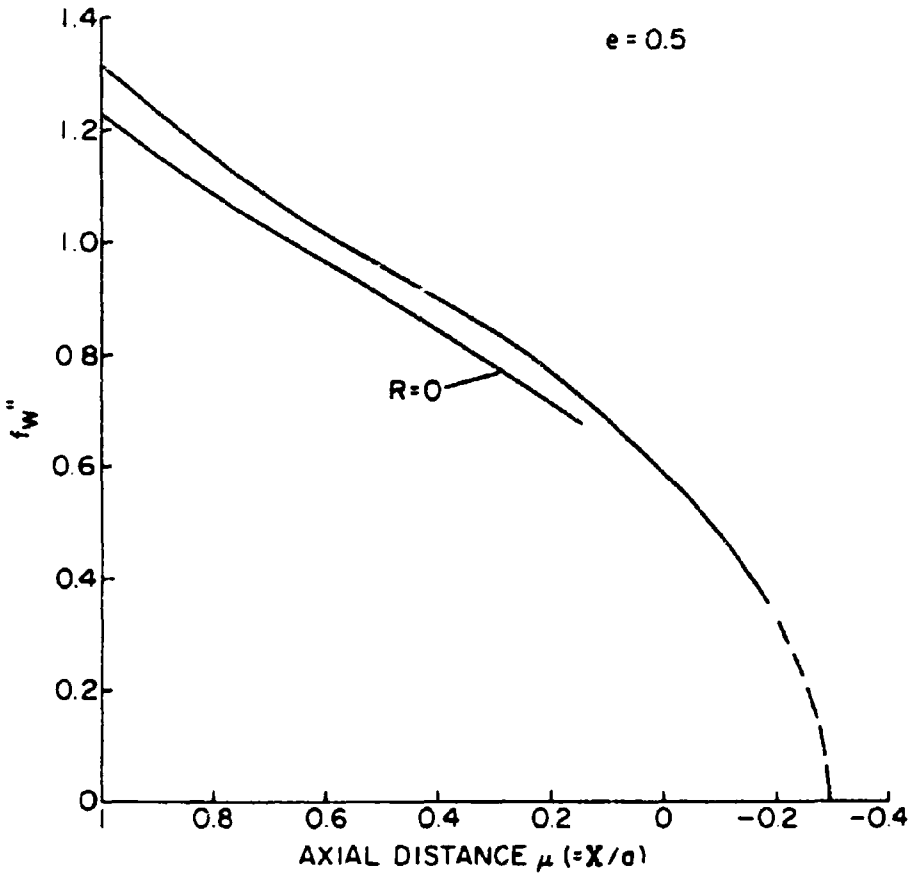

Figure 6 f_w'' for an Ellipsoid

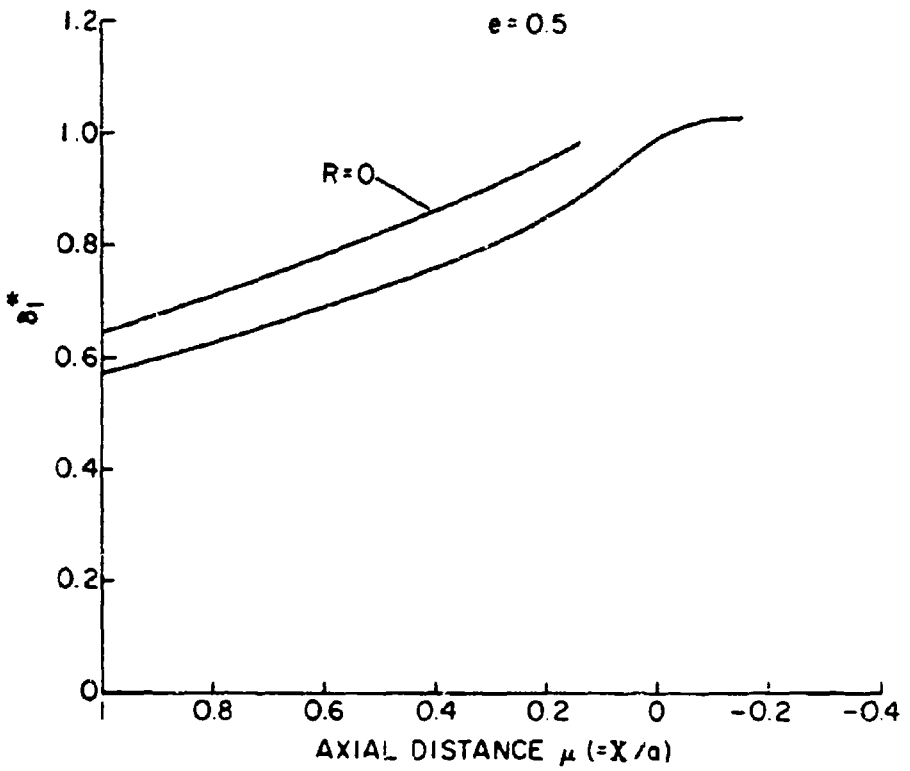

Figure 7 δ_1^* for ar. Ellipsoid

TABLE I

COMPARISON OF VALUES OF f''_w ON A SPHERE AS CALCULATED BY THE PRESENT METHOD AND THE METHOD DUE TO SMITH AND CLUTTER

θ^o	f''_w Present Method	f''_w Smith and Clutter
0	1.31348	1.31189
30	1.26038	1.25888
60	1.07652	1.09011
90	0.63127	0.6562
100	0.34365	0.3580
104[a]	0	———
105.9[a]	———	0

[a]Extrapolated values.

In Figures 8 through 15, the dimensionless terms (20) of the vorticity Equation (13) have been plotted for several longitudinal locations on the sphere and ellipsoid. Here, the effects of each term can be observed and the most important of these is described below.

In the region near the forward stagnation point, the vorticity produced due to stretching is almost exactly equal in magnitude to the u-convection of vorticity as indicated in Figures 8 and 12. This is a result of the fact that near the stagnation point u and ω_θ can be written as:

$$u = cxf'(\eta),$$

and

$$\omega_\theta = -\frac{\partial u}{\partial y} \cong -\frac{c}{\delta} xf'',$$

where c is a constant[12]. In addition, since $r_o \cong x$,

$$\frac{u\omega_\theta}{r_o}\frac{dr_o}{dx} \cong \frac{u\omega_\theta}{x},$$

and, therefore,

$$\frac{u\omega_\theta}{r_o}\frac{dr_o}{dx} \cong \frac{-c^2x}{\delta} f'f'',$$

and

$$u\frac{\partial\omega_\theta}{\partial x} \cong \frac{-c^2x}{\delta} f'f''.$$

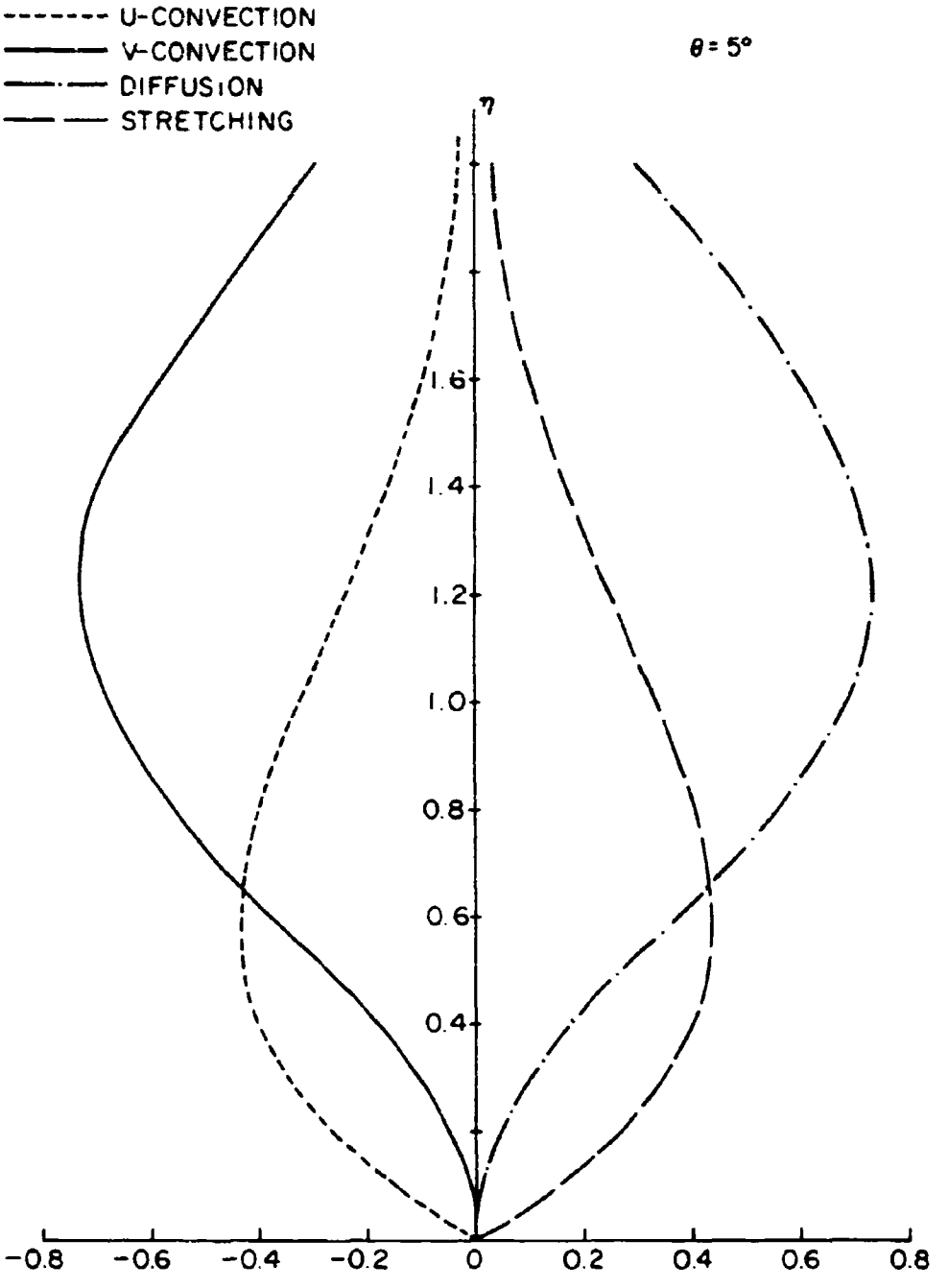

Figure 8 Dimensionless Terms of the Vorticity Equation for a Sphere

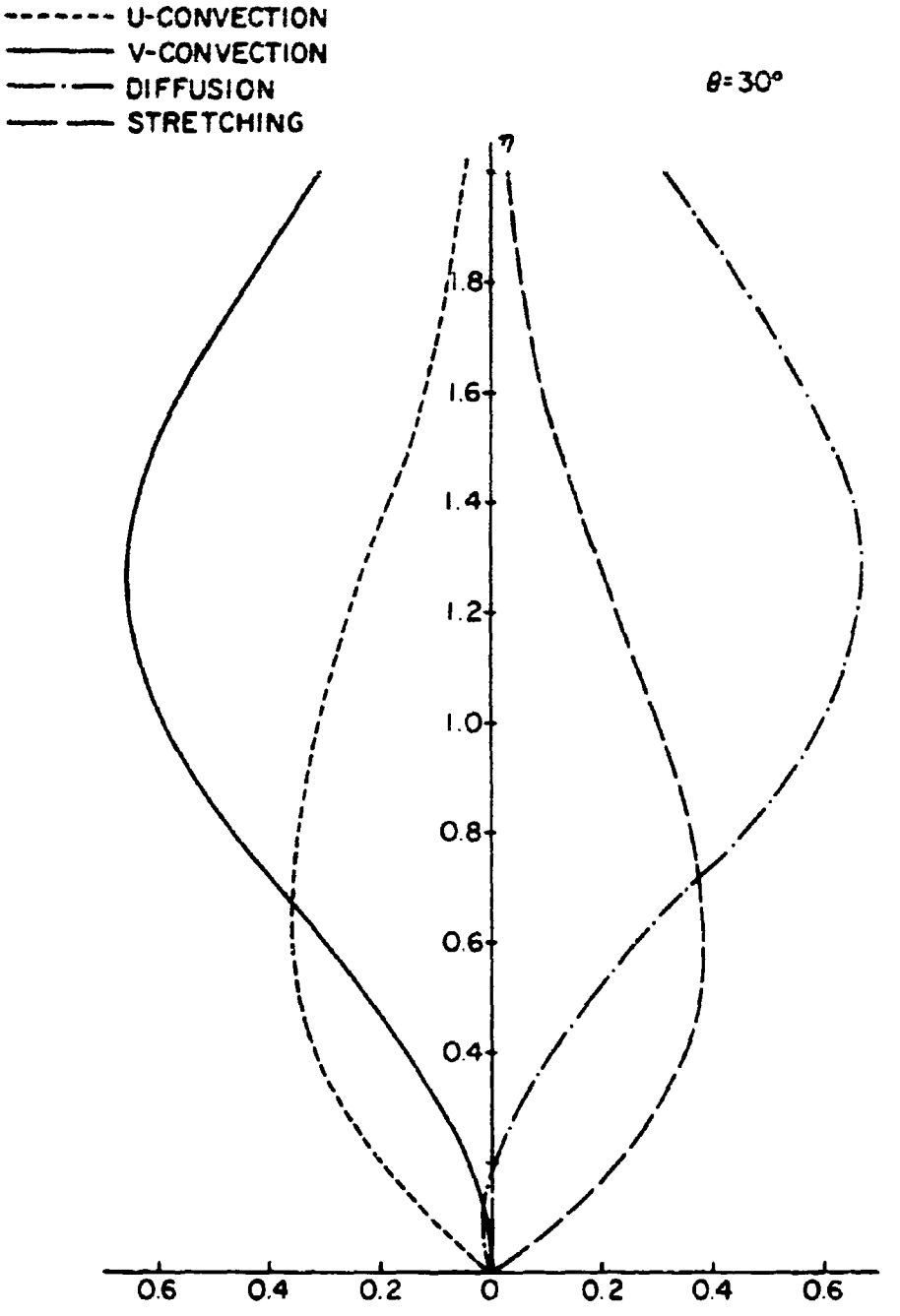

Figure 9 Dimensionless Terms of the Vorticity Equation for a Sphere

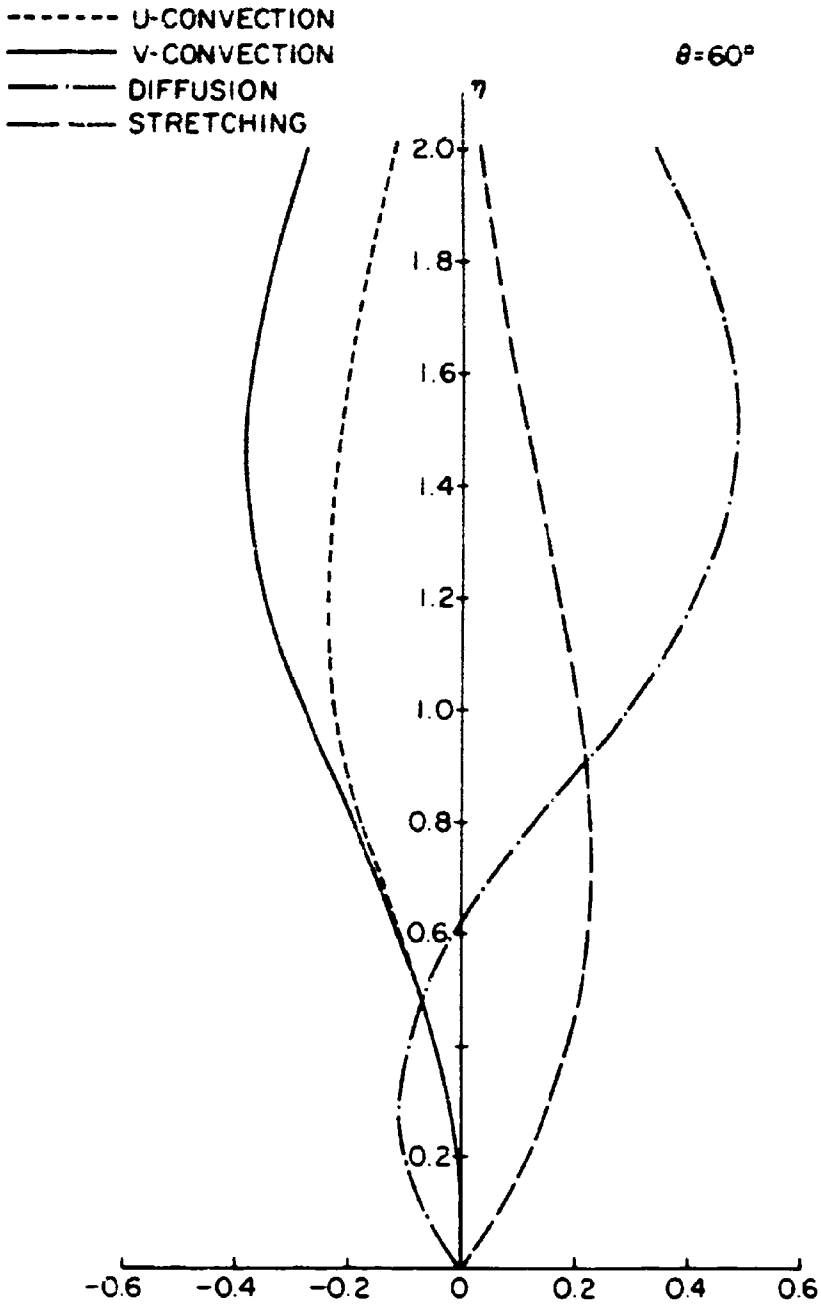

Figure 10 Dimensionless Terms of the Vorticity Equation for a Sphere

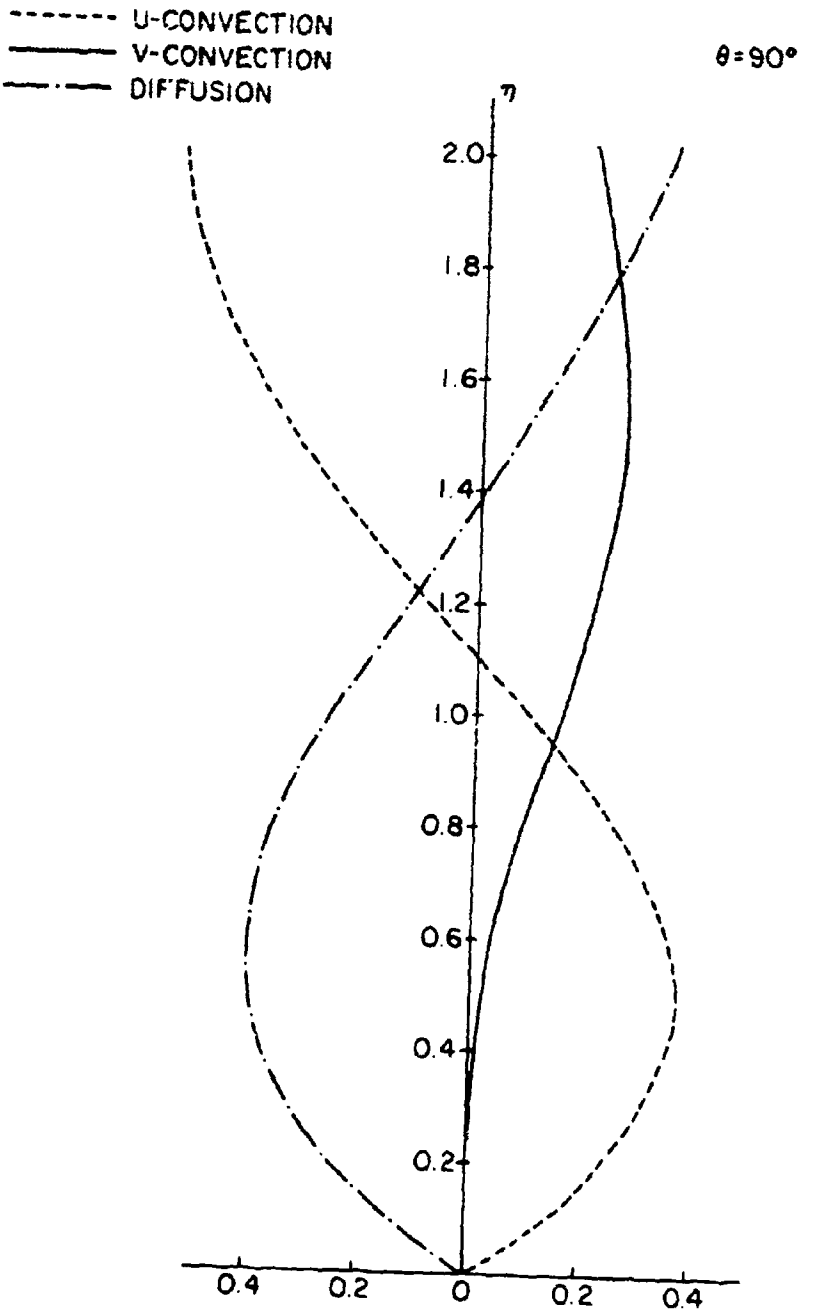

Figure 11 Dimensionless Terms of the Vorticity Equation for a Sphere

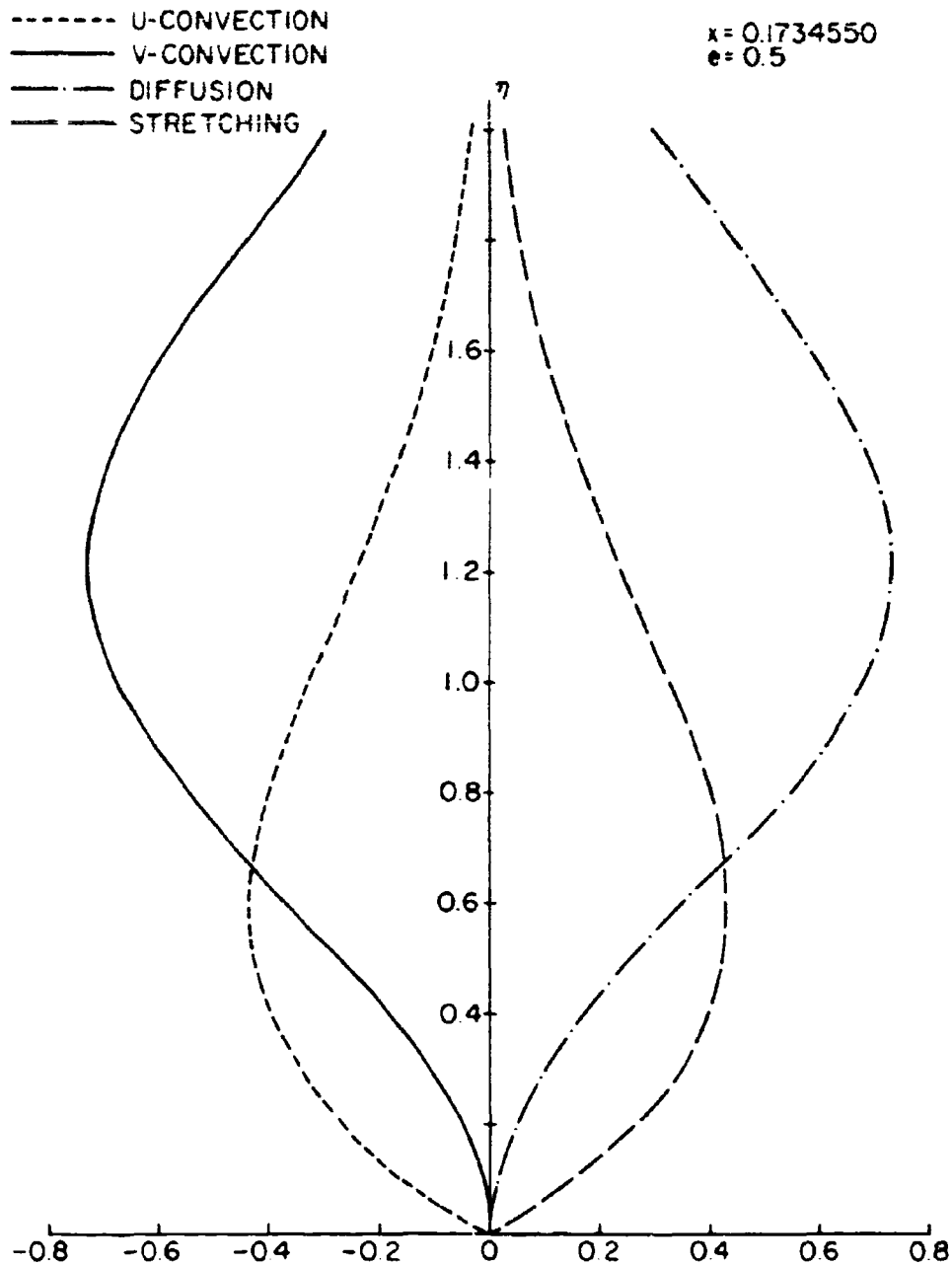

Figure 12 Dimensionless Terms of the Vorticity Equation for an Ellipsoid

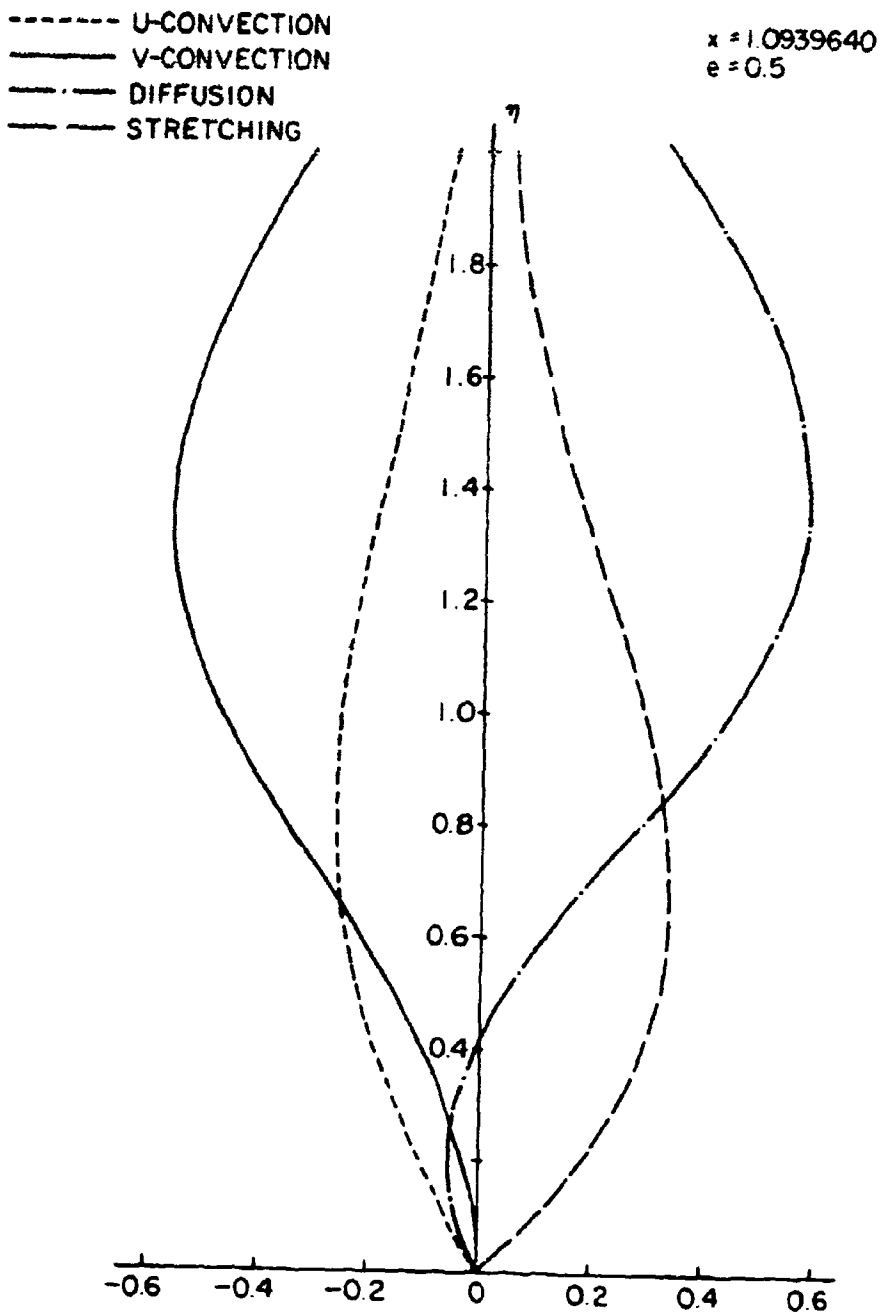

Figure 13 Dimensionless Terms of the Vorticity Equation for an Ellipsoid

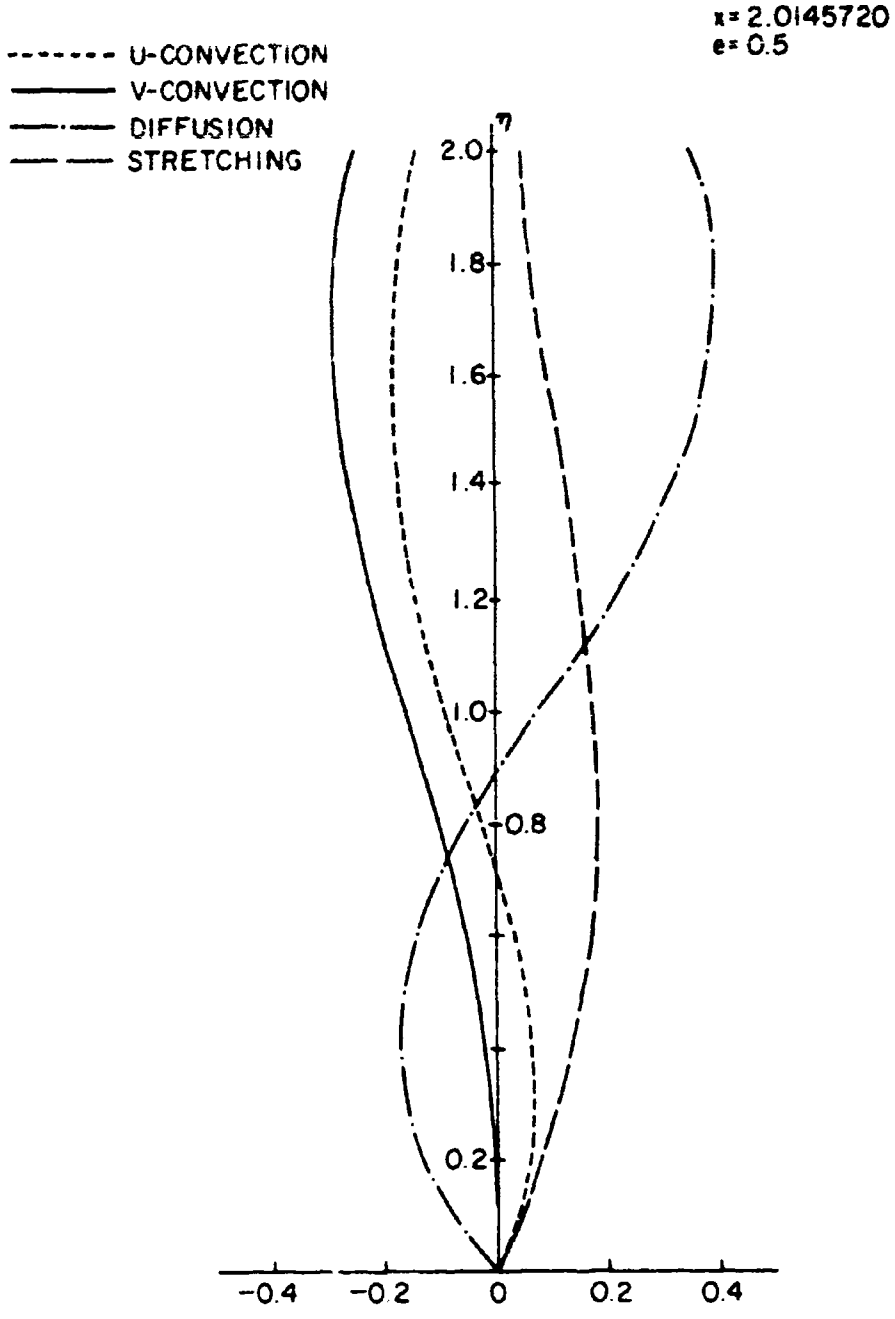

Figure 14 Dimensionless Terms of the Vorticity Equation for an Ellipsoid

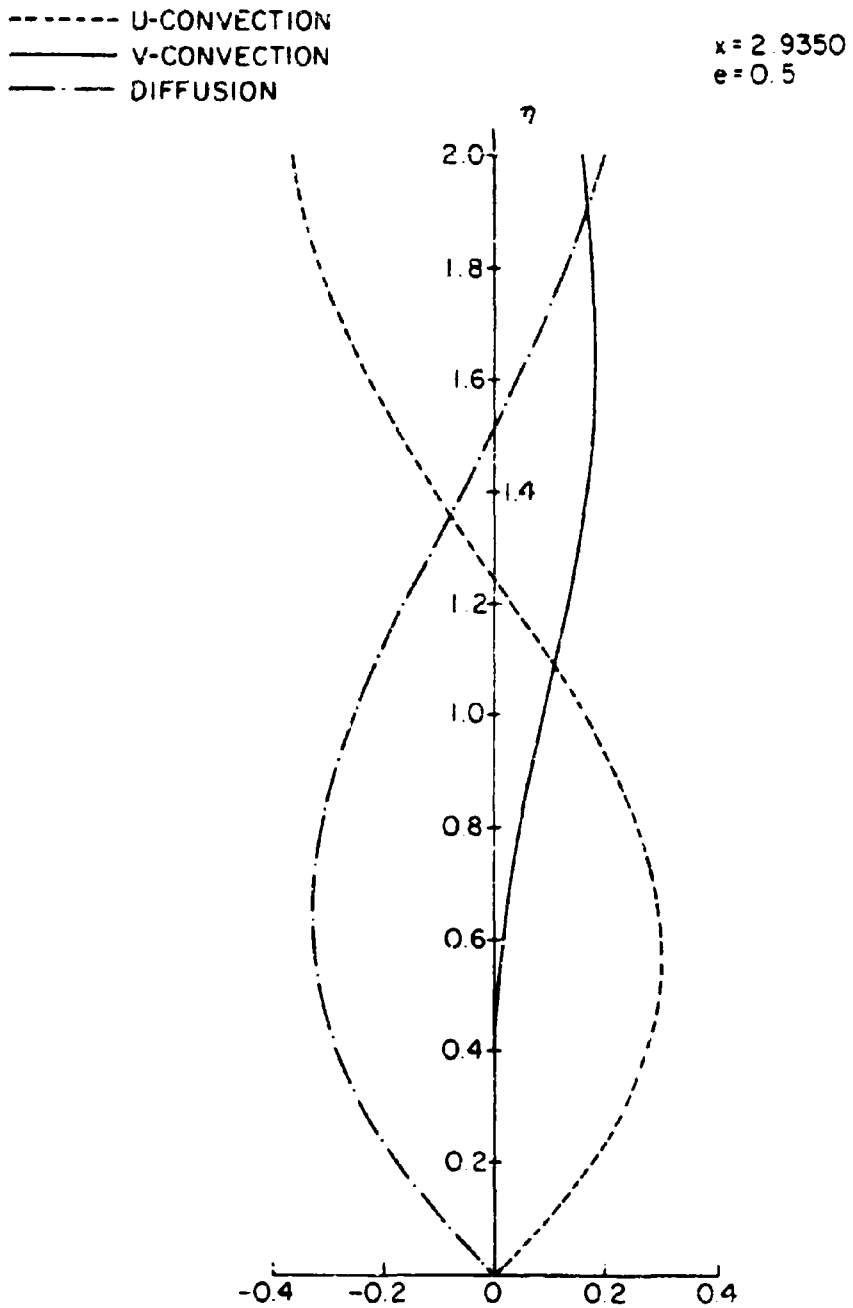

Figure 15 Dimensionless Terms of the Vorticity Equation for an Ellipsoid

Here, the diffusion of the vorticity produced in the lower boundary layer is effectively opposed by the action of convection normal to the surface.

Further downstream, the counteracting effect of diffusion becomes very evident (Figures 10 and 14). Since

$$\frac{1}{\rho}\left(\frac{\partial \tau}{\partial y}\right)_w = \frac{1}{\rho}\frac{\partial p}{\partial x} ,$$

from Equations (2) and (15), it is easily seen that

$$\nu\left(\frac{\partial \omega_\theta}{\partial y}\right)_w = -\frac{1}{\rho}\frac{\partial p}{\partial x} . \qquad (32)$$

So, from Equation (32), the integrated diffusion term is proportional to the pressure gradient. Now, since $\partial p/\partial x$ is negative due to the acceleration of the external stream, it is apparent that diffusion is becoming predominant and the vorticity production in the lower boundary layer (stretching) is transported away entirely by diffusion to higher levels.

Conclusions

The principal results and conclusions obtained from this study are summarized by the following statements:

1) A computer program was successfully developed to solve the incompressible laminar boundary layer equations for the case of steady flow at high Reynolds number about blunt-nosed bodies of revolution where there are no large variations in longitudinal curvature. The method appears to provide sufficient numerical accuracy for most engineering applications except near flow separation where the accuracy falls to about two decimal places (cf. Table 1). Lastly, the program is capable of providing solutions rapidly, since the total execution time was under three minutes for either the sphere or the ellipsoid.

2) The local tendency of large vorticity production in the lower boundary layer creates larger curvature of the vorticity distribution in the middle boundary layer. Therefore, there is more rapid diffusion which increases the boundary layer growth and counteracts the trend towards large values of

vorticity at the wall. Hence, ω_θ is increased by only a small percentage, even though the local stretching effect can be very large.

3) Vortex stretching tends to produce a greater increase in vorticity in a region close to the surface. Consequently, skin friction is increased, creating more rapid growth of the boundary layer which, in turn, tends to inhibit the increase in skin friction.

APPENDIX A

COMPUTER PROGRAM FOR SOLVING THE BOUNDARY LAYER EQUATIONS

The following computer program was written in the Fortran IV G language for the IBM 360/67 digital computer of the Computation Center at The Pennsylvania State University. A detailed discussion of the method used can be found in Chapter III.

```
C      COMPUTER PROGRAM FOR SOLVING THE BOUNDARY LAYER EQUATIONS
       REAL K
       DIMENSION X1(505),X2(505),X3(505),X4(505),X5(3),SOL1(3),SOL2(3),SO
      1L3(3),PREV0(25,505),PREV1(25,505),LW(300),PI(100),PPI(100),PDI(100
      2),PTI(100),XYZ(300),EPS1(25),EPS2(25),ST(400),UV(25),TA(3),TB(3),V
      3EL(505),FSLN(505)
       INTEGER MM(450)
       DATA X1/5*0./,X2/5*0./,X3/5*0./,X4/5*0./
       PIA(A,B,C,D,E,F,G,H) = A*(B-1.)-C*(D-E)+F*(G+H)
       PPIA(A,B,C,D,E,F) = -1.+A*(B+C)-D*(E-F)
       PDIA(A,B,C,D) = A+B*(C+D)
       BETA1(A,B,C,D,E,F,G,X,Y,Z) = A+B*C+D*E+F*(188.*G-123.*X+72.*Y-17.*
      1Z)
       BETA2(A,B,C,D,E,F,G,X) = A+B*C+D*(323.*E-264.*F+159.*G-38.*X)
       BETA3(A,B,C,D,E,F) = A+B*(55.*C-59.*D+37.*E-9.*F)
       ZETA1(A,B,C,D,E,F,G,X,Y,Z) = A+B*C+D*E+F*(17.*G+120.*X-21.*Y+4.*Z)
       ZETA2(A,B,C,D,E,F,G,X) = A+B*C+D*(38.*E+171.*F-36.*G+7.*X)
       ZETA3(A,B,C,D,E,F) = A+B*(9.*C+19.*D-5.*E+F)
       READ 500,K,PHIDPW,ETAINF,H,P,A1,S1,LIM,STUPID
       READ 501,(EPS1(MZ),MZ=1,LIM)
       READ 501,(EPS2(NZ),NZ=1,LIM)
       READ 502,ICK,CK1,CK2,MESS,LOGM,LOGN,LOGO
       READ 505,(UV(JL),JL=1,LIM)
       READ 506,(TA(LAT),LAT=1,3),(TB(LBT),LBT=1,3)
       X2(1) = -1.
       X3(1) = PHIDPW
       FINANS = X3(1)
       XYZ(1) = 10000.
       FSLN(1) = 0.
       LSO = 0
       LC = 0
       H1 = H/4.
       ETA1 = H1
       H1HALF = .5*H1
       H1SQ = H1HALF*H1
       H1SQ1 = .2*H1SQ
       H1CUB = H1*H1SQ1/12.
       HD = H/24.
       HSQ = .5*H*H
       HCUR = HSQ*H/360.
       HSQ1 = HSQ/180.
       DO 24 LAM = 1,LIM
       ICOUNT = 0
       CALL IDIOT(K,P,TA,TB,LAM,LOGM,LOGN,LOGO)
       IF(LAM-MESS) 23,900,900
   900 LC = 1
    23 LS = 0
       IH = 1
       IL = 1
       MIN = 1
       IX = 1
       MST = 1
       X4(1) = -EPS1(LAM)
       ST(1) = X3(1)
       MM(1) = 0
       LW(1) = 0
    11 P1 = -H1+H1SQ*X3(1)+(H1*H1SQ/3.)*X4(1)
       PPR1 = -1.+H1*X3(1)+H1SQ*X4(1)
       PDPR1 = X3(1)+H1*X4(1)
       PTPR1 = TRIP(PREV0,PREV1,LAM,EPS1(LAM),ETA1,2,P1,PPR1,PDPR1,EPS2(L
```

```
     1AM),LC,UV)
      PI(1) = PIA(H1HALF,PPR1,H1SQ1,PDPR1,X3(1),H1CUB,PTPR1,X4(1))
      PPI(1) = PPIA(H1HALF,PDPR1,X3(1),H1SQ1,PTPR1,X4(1))
      PDI(1) = PDIA(X3(1),H1HALF,PTPR1,X4(1))
      PTI(1) = TRIP(PREV0,PREV1,LAM,EPS1(LAM),ETA1,2,PI(1),PPI(1),PDI(1)
     1,EPS2(LAM),LC,UV)
      ICOUNT = ICOUNT+1
      I = 2
    1 J = I-1
      PI(I) = PIA(H1HALF,PPR1,H1SQ1,PDPR1,X3(1),H1CUB,PTI(J),X4(1))
      PPI(I) = PPIA(H1HALF,PDPR1,X3(1),H1SQ1,PTI(J),X4(1))
      PDI(I) = PDIA(X3(1),H1HALF,PTI(J),X4(1))
      PTI(I) = TRIP(PREV0,PREV1,LAM,EPS1(LAM),ETA1,2,PI(I),PPI(I),PDI(I)
     1,EPS2(LAM),LC,UV)
      IF(ABS(PTI(I)-PTI(J)).LE.CK1) GO TO 2
      I = I+1
      GO TO 1
    2 ETA = ETA1
      X1(2) = PI(I)
      X2(2) = PPI(I)
      X3(2) = PDI(I)
      X4(2) = PTI(I)
      CALL STAMCH(PREV0,PREV1,X1(2),X2(2),X3(2),X4(2),ETA,H1,EPS1(LAM),L
     1AM,X1(5),X2(5),X3(5),X4(5),X4(4),X4(3),X1(4),X1(3),X2(4),X2(3),EPS
     22(LAM),X4(1),CK2,LC,UV,X3(3),X3(4),FSLN)
      NM = 6
      ETA = H
      ITILT = 0
    3 ETA = ETA+H
      KK = NM-1
      KX = NM-2
      KY = NM-3
      KZ = NM-4
      Y1 = BETA1(X1(KK),H,X2(KK),HSQ,X3(KK),HCUB,X4(KK),X4(KX),X4(KY),X4
     1(KZ))
      Y2 = BETA2(X2(KK),H,X3(KK),HSQ1,X4(KK),X4(KX),X4(KY),X4(KZ))
      Y3 = BETA3(X3(KK),HD,X4(KK),X4(KX),X4(KY),X4(KZ))
      Y4 = TRIP(PREV0,PREV1,LAM,EPS1(LAM),ETA,NM,Y1,Y2,Y3,EPS2(LAM),LC,U
     1V)
      X1(NM) = ZETA1(X1(KK),H,X2(KK),HSQ,X3(KK),HCUB,Y4,X4(KK),X4(KX),X4
     1(KY))
      X2(NM) = ZETA2(X2(KK),H,X3(KK),HSQ1,Y4,X4(KK),X4(KX),X4(KY))
      X3(NM) = ZETA3(X3(KK),HD,Y4,X4(KK),X4(KX),X4(KY))
      X4(NM) = TRIP(PREV0,PREV1,LAM,EPS1(LAM),ETA,NM,X1(NM),X2(NM),X3(NM
     1),EPS2(LAM),LC,UV)
      IF(ITILT.EQ.1) GO TO 32
      IF(X2(NM).GT.-K) GO TO 31
      IF(ETA.LT.ETAINF) GO TO 930
      IX = IX+1
      XYZ(IX) = ABS(X2(NM))
      IF(XYZ(IX).GE.XYZ(IX-1)) GO TO 6020
      XLW = X3(1)
      MIN = MIN+1
 6020 X3(1) = X3(1)+.025
      GO TO 6
  930 IF(ABS(X2(NM)).LE.1.) GO TO 932
      X3(1) = .5*(HIGH+X3(1))
      GO TO 777
  932 NM = NM+1
      GO TO 3
```

```
 31 ITILT = 1
 32 IF(X2(NM).GT.P) GO TO 4
    IF(X2(NM).LT.-K) GO TO 5
    IF(ETA.GE.ETAINF) GO TO 8
    NM = NM+1
    GO TO 3
  4 IH = IH+1
    HH(IH) = NM
    IF(HH(IH).LE.HH(IH-1)) GO TO 41
    HIGH = X3(1)
 41 X3(1) = X3(1)-S1
    GO TO 6
  5 IL = IL+1
    MIN = MIN+1
    LW(IL) = NM
    IF(LW(IL).LE.LW(IL-1)) GO TO 51
    XLW = X3(1)
 51 X3(1) = X3(1)+A1
  6 IF(X3(1)) 301,66,66
 66 IF(IH.GT.1.AND.MIN.GT.1) GO TO 7
    GO TO 11
  7 X3(1) = .5*(HIGH+XLW)
777 MST = MST+1
    ST(MST) = X3(1)
    IF(ST(MST).EQ.ST(MST-1)) CALL CHGETA(ETAINF,X3(1),E23,E25,FINANS,L
   1SD,STUPID,ICK)
    GO TO 11
  8 LS = LS+1
    SOL3(LS) = X3(NM)
    SOL1(LS) = X1(NM)
    SOL2(LS) = X2(NM)
    X5(LS) = X3(1)
    IF(LS.EQ.3) GO TO 10
    IF(SOL2(LS).GT.0.) GO TO 9
    X3(1) = .5*(X5(LS)+HIGH)
    GO TO 11
  9 X3(1) = .5*(X5(LS)+XLW)
    GO TO 11
 10 IF(SOL2(1)-SOL2(2)) 9865,9864,9865
9864 IF(SOL2(1)-SOL2(3)) 9865,9866,9865
9866 IF(SOL2(2)-SOL2(3)) 9865,9868,9865
9868 FINANS = X5(1)
    GO TO 200
9865 FINANS = DECIDE(X5,SOL2)
 200 PRINT 2000
    PRINT 2100,(SOL1(LLS),SOL2(LLS),SOL3(LLS),X5(LLS),LLS=1,3)
    PRINT 2200,FINANS,LAM,ETAINF,LSD
    X3(1) = FINANS
    PREVO(LAM,1) = 0.
    PREV1(LAM,1) = -1.
    AP1 = -H1+H1SQ*X3(1)+(H1*H1SQ/3.)*X4(1)
    APPR1 = -1.+H1*X3(1)+H1SQ*X4(1)
    APDPR1 = X3(1)+H1*X4(1)
    APTPR1 = TRIP(PREVO,PREV1,LAM,EPS1(LAM),ETA1,2,AP1,APPR1,APDPR1,EP
   1S2(LAM),LC,UV)
    PI(1) = PIA(H1HALF,APPR1,H1SQ1,APDPR1,X3(1),H1CUB,APTPR1,X4(1))
    PPI(1) = PPIA(H1HALF,APDPR1,X3(1),H1SQ1,APTPR1,X4(1))
    PDI(1) = PDIA(X3(1),H1HALF,APTPR1,X4(1))
    PTI(1) = TRIP(PREVO,PREV1,LAM,EPS1(LAM),ETA1,2,PI(1),PPI(1),PDI(1)
   1,EPS2(LAM),LC,UV)
```

```
      L = 2
  201 LJ = L-1
      PI(L) = PIA(H1HALF,APPR1,H1SQ1,APOPR1,X3(1),H1CUB,PTI(LJ),X4(1))
      PPI(L) = PPIA(H1HALF,APOPR1,X3(1),H1SQ1,PTI(LJ),X4(1))
      PDI(L) = PDIA(X3(1),H1HALF,PTI(LJ),X4(1))
      PTI(L) = TRIP(PREV0,PREV1,LAM,EPS1(LAM),ETA1,2,PI(L),PPI(L),PDI(L)
     1,EPS2(LAM),LC,UV)
      IF(ABS(PTI(L)-PTI(LJ)).LE.CK1) GO TO 202
      L = L+1
      GO TO 201
  202 ETA = ETA1
      X1(2) = PI(L)
      FSLN(2) = X1(2)+ETA
      X2(2)= PPI(L)
      X3(2) = PDI(L)
      X4(2) = PTI(L)
      PREV0(LAM,2) = PI(L)
      PREV1(LAM,2) = PPI(L)
      CALL STAMCH(PREV0,PREV1,X1(2),X2(2),X3(2),X4(2),ETA,H1,EPS1(LAM),L
     1AM,X1(5),X2(5),X3(5),X4(5),X4(4),X4(3),X1(4),X1(3),X2(4),X2(3),EPS
     22(LAM),X4(1),CK2,LC,UV,X3(3),X3(4),FSLN)
      LNM = 6
      ETA = H
  203 ETA = ETA+H
      LKK = LNM-1
      LKX = LNM-2
      LKY = LNM-3
      LKZ = LNM-4
      Y1 = BETA1(X1(LKK),H,X2(LKK),HSQ,X3(LKK),HCUB,X4(LKK),X4(LKX),X4(L
     1KY),X4(LKZ))
      Y2 = BETA2(X2(LKK),H,X3(LKK),HSQ1,X4(LKK),X4(LKX),X4(LKY),X4(LKZ))
      Y3 = BETA3(X3(LKK),HD,X4(LKK),X4(LKX),X4(LKY),X4(LKZ))
      Y4 = TRIP(PREV0,PREV1,LAM,EPS1(LAM),ETA,LNM,Y1,Y2,Y3,EPS2(LAM),LC,
     1UV)
      X1(LNM) = ZETA1(X1(LKK),H,X2(LKK),HSQ,X3(LKK),HCUB,Y4,X4(LKK),X4(L
     1KX),X4(LKY))
      FSLN(LNM) = X1(LNM)+ETA
      X2(LNM) = ZETA2(X2(LKK),H,X3(LKK),HSQ1,Y4,X4(LKK),X4(LKX),X4(LKY))
      PREV0(LAM,LNM) = X1(LNM)
      PREV1(LAM,LNM) = X2(LNM)
      X3(LNM) =ZETA3(X3(LKK),HD,Y4,X4(LKK),X4(LKX),X4(LKY))
      X4(LNM) = TRIP(PREV0,PREV1,LAM,EPS1(LAM),ETA,LNM,X1(LNM),X2(LNM),X
     13(LNM),EPS2(LAM),LC,UV)
      IF(ETA.GE.ETAINF) GO TO 204
      LNM = LNM+1
      GO TO 203
  204 PRINT 504,X2(LNM),X3(LNM)
      PRINT 4000,ICOUNT,UV(LAM)
      DISPL = -X1(LNM)
      DO 400 IKW = 1,LNM
  400 VEL(IKW) = X2(IKW)+1.
      PRINT 5000
      PRINT 5001,(VEL(IKZ),IKZ=1,LNM)
      PRINT 5002,DISPL
      PRINT 5003
      PRINT 5004,(X3(LKW),LKW=1,LNM)
      PRINT 5005
      PRINT 5006,(FSLN(LZZ),LZZ=1,LNM)
      PRINT 5007
      PRINT 5008,(X4(LBG),LBG=1,LNM)
```

```
  24 CONTINUE
     GO TO 25
 301 PRINT 503,X3(I),LAM
  25 STOP
 500 FORMAT(7F10.7,I3,F5.2)
 501 FORMAT(5F12.8)
 502 FORMAT(I10,2F12.8,I10,3I3)
 503 FORMAT('0','A NEGATIVE TRIAL VALUE FOR WALL SHEAR = ',F14.8,' OCCU
    1RRED AT LAM = ',I4)
 504 FORMAT(' ','AT INFINITY  X2 = ',F14.8,' AND X3 = ',F14.8)
 505 FORMAT(6F12.6)
 506 FORMAT(6F10.7)
2000 FORMAT('0',7X,'SOL1',16X,'SOL2',15X,'SOL3',12X,'X5')
2100 FORMAT(' ',4(F14.8,5X))
2200 FORMAT('0','FINANS = ',F14.8,5X,'FOR LAM = ',I3,5X,'ETAINF = ',F14
    1.7,5X,'TOTAL NO. OF CHANGES IN ETAINF = ',I4)
4000 FORMAT('0','ICOUNT = ',I4,5X,'FOR THETA = ',F12.6,' DEGREES')
5000 FORMAT('0','THE VELOCITY PROFILE IS')
5001 FORMAT(' ',11F11.7)
5002 FORMAT('0','THE NON DIMENSIONAL DISPLACEMENT THICKNESS IS',F12.7)
5003 FORMAT('0','THE VELOCITY GRADIENT PROFILE IS')
5004 FORMAT(' ',11F11.7)
5005 FORMAT('0','THE SOLUTION PROFILE FOR F IS')
5006 FORMAT(' ',11F11.7)
5007 FORMAT('0','THE PROFILE FOR F TRIPLE PRIME IS')
5008 FORMAT(' ',11F11.7)
     END
     SUBROUTINE STAMCH(F,G,AA,BB,CC,DD,E,HO,YM,I,RIO,RI1,RI2,RTI1,XX1,Y
    1Y1,A0,B0,A1,B1,R,W,C,JJ,U,X33,X34,FS)
     DIMENSION F(25,505),G(25,505),PCP(50),PCR(50),PCD(50),STC(50),QI0(
    150),QI1(50),QI2(50),QTI(50),U(25),FS(505)
     INTEGER P
     SIG0(A,B,C,D,E,F,G,X) = A+B*C+D*E+F*(17.*G+120.*X)
     SIG1(A,B,C,D,E,F) = A+B*C+D*(38.*E+171.*F)
     SIG2(A,B,C,D) = A+B*(9.*C+19.*D)
     GAM0(A,B,C,D,E,F,G,X,Y) = A+B*C+D*E+F*(17.*G+120.*X-21.*Y)
     GAM1(A,B,C,D,E,F,G) = A+B*C+D*(38.*E+171.*F-36.*G)
     GAM2(A,B,C,D,E) = A+B*(9.*C+19.*D-5.*E)
     DELT0(A,B,C,D,E,F,G,X,Y,Z) = A+B*C+D*E+F*(17.*G+120.*X-21.*Y+4.*Z)
     DELT1(A,B,C,D,E,F,G,X) = A+B*C+D*(38.*E+171.*F-36.*G+7.*X)
     DELT2(A,B,C,D,E,F) = A+B*(9.*C+19.*D-5.*E+F)
     E = E+HO
     HOD = HO/24.
     HOSQ = HO*HO
     HOSQ1 = .5*HOSQ
     HSQ2 = HOSQ1/180.
     HOCUB = HO*HOSQ/720.
     PHIP1 = AA+HO*BB+HOSQ1*CC+HOCUB*(188.*DD-123.*W)
     PHPP1 = BB+HO*CC+HSQ2*(323.*DD-264.*W)
     PHDP1 =  CC+HOD*(55.*DD-59.*W)
     STP1 = TRIP(F,G,I,YM,E,3,PHIP1,PHPP1,PHDP1,R,JJ,U)
     PCP(1) = SIG0(AA,HO,BB,HOSQ1,CC,HOCUB,STP1,DD)
     PCR(1) = SIG1(BB,HO,CC,HSQ2,STP1,DD)
     PCD(1) = SIG2(CC,HOD,STP1,DD)
     STC(1) = TRIP(F,G,I,YM,E,3,PCP(1),PCR(1),PCD(1),R,JJ,U)
     K = 2
 101 L = K-1
     PCP(K) = SIG0(AA,HO,BB,HOSQ1,CC,HOCUB,STC(L),DD)
     PCR(K) = SIG1(BB,HO,CC,HSQ2,STC(L),DD)
     PCD(K) = SIG2(CC,HOD,STC(L),DD)
```

```
      STC(K) = TRIP(F,G,I,YM,E,3,PCP(K),PCR(K),PCD(K),R,JJ,U)
      IF(ABS(STC(K)-STC(L)).LE.C) GO TO 102
      K = K+1
      GO TO 101
  102 FS(3) = PCP(K)+E
      E = E+HO
      Q0 = PCP(K)+HO*PCR(K)+HOSQ1*PCD(K)+HOCUB*(188.*STC(K)-123.*DD+72.*
     1W)
      Q1 = PCR(K)+HO*PCD(K)+HSQ2*(323.*STC(K)-264.*DD+159.*W)
      Q2 = PCD(K)+HOD*(55.*STC(K)-59.*DD+37.*W)
      QT1 = TRIP(F,G,I,YM,E,4,Q0,Q1,Q2,R,JJ,U)
      QI0(1) = GAM0(PCP(K),HO,PCR(K),HOSQ1,PCD(K),HOCUB,QT1,STC(K),DD)
      QI1(1) = GAM1(PCR(K),HO,PCD(K),HSQ2,QT1,STC(K),DD)
      QI2(1) = GAM2(PCD(K),HOD,QT1,STC(K),DD)
      QTI(1) = TRIP(F,G,I,YM,E,4,QI0(1),QI1(1),QI2(1),R,JJ,U)
      N = 2
  103 P = N-1
      QI0(N) = GAM0(PCP(K),HO,PCR(K),HOSQ1,PCD(K),HOCUB,QTI(P),STC(K),DD
     1)
      QI1(N) = GAM1(PCR(K),HO,PCD(K),HSQ2,QTI(P),STC(K),DD)
      QI2(N) = GAM2(PCD(K),HOD,QTI(P),STC(K),DD)
      QTI(N) = TRIP(F,G,I,YM,E,4,QI0(N),QI1(N),QI2(N),R,JJ,U)
      IF(ABS(QTI(N)-QTI(P)).LE.C) GO TO 104
      N = N+1
      GO TO 103
  104 FS(4) = QI0(N)+E
      E = E+HO
      R0 = QI0(N)+HO*QI1(N)+HOSQ1*QI2(N)+HOCUB*(188.*QTI(N)-123.*STC(K)+
     172.*DD-17.*W)
      R1 = QI1(N)+HO*QI2(N)+HSQ2*(323.*QTI(N)-264.*STC(K)+159.*DD-38.*W)
      R2 = QI2(N)+HOD*(55.*QTI(N)-59.*STC(K)+37.*DD-9.*W)
      RT1 = TRIP(F,G,I,YM,E,5,R0,R1,R2,R,JJ,U)
      RI0 = DELT0(QI0(N),HO,QI1(N),HOSQ1,QI2(N),HOCUB,RT1,QTI(N),STC(K),
     1DD)
      RI1 = DELT1(QI1(N),HO,QI2(N),HSQ2,RT1,QTI(N),STC(K),DD)
      RI2 = DELT2(QI2(N),HOD,RT1,QTI(N),STC(K),DD)
      RTI1 = TRIP(F,G,I,YM,E,5,RI0,RI1,RI2,R,JJ,U)
      FS(5) = RI0+E
      XX1 = QTI(N)
      YY1 = STC(K)
      A0 = QI0(N)
      B0 = PCP(K)
      A1 = QI1(N)
      B1 = PCR(K)
      X33 = PCD(K)
      X34 = QI2(N)
      F(I,3) = B0
      F(I,4) = A0
      F(I,5) = RI0
      G(I,3) = B1
      G(I,4) = A1
      G(I,5) = RI1
      RETURN
      END
      SUBROUTINE CHGETA(X,Y,*,*,Z,I,U,J)
      I = I+1
      IF(I.GT.J) GO TO 20
      X = X-U
      Y = Z
      RETURN 1
```

```
   20 PRINT 8000
      RETURN 2
 8000 FORMAT('0','FAILURE')
      END
      SUBROUTINE IDIOT(X,Y,A,B,L,M,N,JO)
      DIMENSION A(3),B(3)
      IF(L-M) 1,2,2
    2 IF(L-N) 3,4,4
    3 X = A(1)
      Y = B(1)
      GO TO 1
    4 IF(L-JO) 5,6,6
    5 X = A(2)
      Y = B(2)
      GO TO 1
    6 X = A(3)
      Y = B(3)
    1 RETURN
      END
      FUNCTION DECID(X,Y)
      DIMENSION X(3),Y(3),P(3),S(3),IXP(3),IXS(3)
      IJP = 0
      IKS = 0
      J = 0
      BPOS = 1.
      K = 0
      BNEG = 1.
      DO 5 I = 1,3
      IF(Y(I)) 3,5,1
    1 J = J+1
      P(J) = Y(I)
      IXP(J) = I
      IF(P(J)-BPOS) 2,5,5
    2 BPOS = P(J)
      JJ = IXP(J)
      IJP = 1
      GO TO 5
    3 K = K+1
      S(K) = ABS(Y(I))
      IXS(K) = I
      IF(S(K)-BNEG) 4,5,5
    4 BNEG = S(K)
      KK = IXS(K)
      IKS = 1
    5 CONTINUE
      IF(IJP.EQ.1) GO TO 6
      DECID = X(KK)
      GO TO 111
    6 IF(IKS.EQ.1) GO TO 7
      DECID = X(JJ)
      GO TO 111
    7 IF(ABS(X(JJ)-X(KK))-.0000001) 13,13,77
   13 IF(BPOS-BNEG) 131,131,133
  131 DECID = X(JJ)
      GO TO 111
  133 DECID = X(KK)
      GO TO 111
   77 IF(BPOS-BNEG) 8,9,10
    8 R = BNEG/BPOS
      RAT = AINT(R)
```

```
      DECID = (RAT*X(JJ)+X(KK))/(RAT+1.)
      GO TO 111
    9 DECID = .5*(X(JJ)+X(KK))
      GO TO 111
   10 R = BPOS/BNEG
      RAT = AINT(R)
      DECID = (RAT*X(KK)+X(JJ))/(RAT+1.)
  111 RETURN
      END
      FUNCTION TRIP(X,Y,J,XM,T,K,A,B,C,R,N,S)
      DIMENSION X(25,505),Y(25,505),S(25)
      Z = -(.5*(XM+1.)+R)*(A+T)*C+XM*(B*B+2.*B)
      IF(J.GT.3) GO TO 704
      GO TO (701,702,703),J
  701 TRIP = Z
      GO TO 705
  702 TRIP = Z+((B+1.)*(B-Y(1,K))-C*(A-X(1,K)))
      GO TO 705
  703 F0 = S(J)*(2.*S(J)-S(J-2)-S(J-1))/((S(J)-S(J-2))*(S(J)-S(J-1)))
      F1 = S(J)*(S(J)-S(J-2))/((S(J-1)-S(J-2))*(S(J-1)-S(J)))
      F2 = S(J)*(S(J)-S(J-1))/((S(J-2)-S(J-1))*(S(J-2)-S(J)))
      TRIP = Z+(B+1.)*(F0*B+F1*Y(2,K)+F2*Y(1,K))-C*(F0*A+F1*X(2,K)+F2*X(
     11,K))
      GO TO 705
  704 Q = S(J)*((S(J)-S(J-2))*(S(J)-S(J-1)))/((S(J-3)-S(J-2))*(S(J-3)-S(
     1J-1))*(S(J-3)-S(J)))
      U = S(J)*((S(J)-S(J-3))*(S(J)-S(J-1)))/((S(J-2)-S(J-3))*(S(J-2)-S(
     1J-1))*(S(J-2)-S(J)))
      V = S(J)*((S(J)-S(J-3))*(S(J)-S(J-2)))/((S(J-1)-S(J-3))*(S(J-1)-S(
     1J-2))*(S(J-1)-S(J)))
      W =S(J)*((S(J)-S(J-3))*(S(J)-S(J-2))+(S(J)-S(J-3))*(S(J)-S(J-1))+(
     1S(J)-S(J-2))*(S(J)-S(J-1)))/((S(J)-S(J-3))*(S(J)-S(J-2))*(S(J)-S(J
     2-1)))
      TRIP = Z+(B+1.)*(W*B+V*Y(J-1,K)+U*Y(J-2,K)+Q*Y(J-3,K))-C*(W*A+V*X(
     1J-1,K)+U*X(J-2,K)+Q*X(J-3,K))
  705 RETURN
      END
```

The input data necessary for the proper execution of the above program should consist of the following:

1) The first data card should contain values for $+\varepsilon$, an initial guess for f''_w, η_∞, the η-step size (h), $-\varepsilon$, a_3, a_2, the number of x-steps and the increment by which η_∞ is lowered. (See pages 21-25)
2) The next set of data cards consists of M and R, in that order. These are obtained from the potential flow and body geometry for the particular body under consideration. (See Appendix B)
3) The next data card consists of the maximum number of allowable changes in η_∞, two tolerances for determining numerical equality (1×10^{-7} for single precision), an approximation for the number of the particular x-station which is nearest to the point of separation, and the numbers of the particular x-steps where the values for $+\varepsilon$ and $-\varepsilon$ are to be changed.
4) The next set of data cards consists of the numerical values of x (i.e., arc length) at each x-step.
5) The final data card should give the numerical values for $+\varepsilon$ and $-\varepsilon$ at each step where they are to be changed (cf. statement number three above).

```
C     DATA CARDS FOR AN ELLIPSOID WITH E = 0.5
  .0001    1.5         5.0       .05          .0001       .05       .05      16 .05
  1.00000000  0.99272788  0.94342467  0.85928551  0.75483944
  0.64163615  0.52592935  0.40865935  0.28679066  0.15388433
  0.0        -0.18980688 -0.43842162 -0.78208111 -1.28183309
 -2.04716820
  1.00000000  0.99602872  0.96677345  0.91339371  0.83967158
  0.74859599  0.64153677  0.51756752  0.37360031  0.20397939
  0.0        -0.25159604 -0.57112898 -0.99050652 -1.56360003
 -2.38842745
        80  0.0000001   0.0000001          13  3  6  9
    0.0          0.173455     0.480048     0.787165     1.093964     1.400776
    1.707748     2.014572     2.321336     2.628241     2.935000     3.241760
    3.548664     3.855429     4.162251     4.469226
   .0001       .0003       .0005       .0001       .0003       .0005
```

APPENDIX B

CALCULATION OF M AND R FOR AN ELLIPSOID

Coordinate System and Geometric Relations

A semi-elliptic coordinate system is a very convenient representation for obtaining the potential flow solution about an ovary ellipsoid. The defining relations are:

$$X = K\mu\delta,$$

$$Y = K(1-\mu^2)^{\frac{1}{2}}\,(\delta^2-1)^{\frac{1}{2}}\cos\omega, \tag{B1}$$

and

$$Z = K(1-\mu^2)^{\frac{1}{2}}\,(\delta^2-1)^{\frac{1}{2}}\sin\omega,$$

where $-1 \leq \mu \leq 1$ and $1 \leq \delta < \infty$[7]. The surfaces δ = constant, μ = constant are confocal ellipsoids and hyperboloids of two sheets, respectively, with common foci at $(\pm K, 0, 0)$, and ω is taken to be the azimuthal angle in the meridian plane. The coordinates μ, δ, ω form an orthogonal system with the following metric coefficients:

$$h_\mu = K\left(\frac{\delta^2-\mu^2}{1-\mu^2}\right)^{\frac{1}{2}}, \tag{B2}$$

and

$$h_\delta = K\left(\frac{\delta^2-\mu^2}{\delta^2-1}\right)^{\frac{1}{2}}, \tag{B3}$$

and

$$h_\omega = K(1-\mu^2)^{\frac{1}{2}} \ (\delta^2-1)^{\frac{1}{2}} \ . \tag{B4}$$

Considering the meridian plane with Z=0 of the ellipsoid δ_o with semi-major and minor axes a, b, respectively, the following geometric relationships hold:

$$e = \frac{(a^2-b^2)^{\frac{1}{2}}}{a} \ , \tag{B5}$$

and

$$K = ae, \tag{B6}$$

where e is the eccentricity. The equation of the ellipse in the meridian plane is given by the familiar equation:

$$\frac{X^2}{a^2} + \frac{Y^2}{b^2} = 1. \tag{B7}$$

Now, from the relations (B1) with (B5), (B6), and (B7), it is easily proven that for this body (Lamb, 1945):

$$\delta_o = \frac{1}{e} \tag{B8}$$

and

$$\mu = \frac{X}{a} \ . \tag{B9}$$

Calculation of R

Referring to Chapter II, the expression for R can be written as:

$$R = \frac{x}{r_o} \frac{dr_o}{dX} \frac{dX}{dx} . \tag{B10}$$

Now, from well-known formulas of integral calculus, the differential of arc dx and the arc length x are given by:

$$dx = \left[1 + \left(\frac{dY}{dX}\right)^2\right]^{\frac{1}{2}} dX \tag{B11}$$

and

$$x = a\, E\, (e,\mu), \tag{B12}$$

where E (e,μ) is an eiliptic integral of the second kind defined by:

$$E\, (e,\mu) = \int_{\mu}^{1} \left(\frac{1-e^2\mu^2}{1-\mu^2}\right)^{\frac{1}{2}} d\mu. \tag{B13}$$

Since $r_o = Y$, $\frac{dr_o}{dX}$ is readily obtained from (B7) and $\frac{dX}{dx}$ from (B11). Finally, the equation for R becomes:

$$R = \mu E\, (e,\mu) \left[(1-\mu^2)(1-e^2\mu^2)\right]^{-\frac{1}{2}}. \tag{B14}$$

Calculation of M

The velocity potential ϕ for an ellipsoid moving parallel to the X axis is given (see Lamb, 1945) by:

$$\phi = A\mu \left[\tfrac{1}{2}\delta \ln \frac{\delta+1}{\delta-1} - 1 \right] \tag{B15}$$

where $A = aU_\infty \left[\frac{1}{1-e^2} - \frac{1}{2e} \ln \frac{1+e}{1-e} \right]^{-1}$.

From (B15) and (B2), the velocity in the μ direction V_μ is:

$$V_\mu = -\frac{1}{h_\mu}\frac{\partial \phi}{\partial \mu} = -\frac{A}{K}\left(\frac{1-\mu^2}{\delta^2-\mu^2}\right)^{\frac{1}{2}} \left[\tfrac{1}{2}\delta \ln \frac{\delta+1}{\delta-1} - 1 \right]. \tag{B16}$$

For the ellipsoid δ = constant = δ_o, the relation for M takes on the following form:

$$M = \left(\frac{x}{V_\mu}\right)_{\delta_o} \left[\frac{\partial V_\mu}{\partial \mu}\frac{d\mu}{dx}\right]_{\delta_o}. \tag{B17}$$

The quantity $\frac{\partial V_\mu}{\partial \mu}$ on δ_o is obtained from (B16) and is found to be:

$$\left(\frac{\partial V_\mu}{\partial \mu}\right)_{\delta_o} = \frac{A}{a}(1-e^2)\,\mu \left[(1-\mu^2)(1-e^2\mu^2)^3\right]^{-\frac{1}{2}} \left[\frac{1}{2e} \ln \frac{1+e}{1-e} - 1\right]. \tag{B18}$$

The expression for $\frac{d\mu}{dx}$ on δ_o is most conveniently established by differentiating the coordinate relations (B1) and solving the resulting set of simultaneous equations algebraically. The result is:

$$\left(\frac{d\mu}{dx}\right)_{\delta_o} = -\frac{1}{a}\left(\frac{1-\mu^2}{1-e^2\mu^2}\right)^{\frac{1}{2}}. \qquad (B19)$$

After making the appropriate substitutions into (B17), M finally becomes:

$$M = (1-e^2)\ \mu E\ (e,\mu)\left[(1-\mu^2)(1-e^2\mu^2)^3\right]^{-\frac{1}{2}}. \qquad (B20)$$

REFERENCES

1. Batchelor, G. K., An Introduction to Fluid Dynamics, (Cambridge University Press, Cambridge, 1967), pp. 266-343.

2. Collatz, L., The Numerical Treatment of Differential Equations, 3rd edition, (Springer Verlag, Berlin, 1960).

3. Conte, S. D., Elementary Numerical Analysis, (McGraw-Hill Book Company, New York, 1965), pp. 71-110.

4. Goldstein, S., Modern Developments in Fluid Dynamics, Vol. I, Secs. 51 and 64, (Dover Publications, Inc., New York, 1965).

5. Hartree, D. R. and Womersley, J. R., "A Method for the Numerical or Mechanical Solution of Certain Types of Partial Differential Equations," Proc. Royal Soc. Series A, Vol. 161, August 1937, p. 353.

6. Hildebrand, F. B., Introduction to Numerical Analysis, (McGraw-Hill Book Company, New York, 1956).

7. Lamb, Horace, Hydrodynamics, 6th edition, (Dover Publications, Inc., New York, 1945), pp. 139-141.

8. Meksyn, D., New Methods in Laminar Boundary Layer Theory, 1st edition, (Pergamon Press, Oxford, 1961).

9. Narasimha, Roddam and Ojha, S. K., "Effect of Longitudinal Surface Curvature on Boundary Layers," Journal of Fluid Mechanics, Vol. 29, Part 1, July 1967, p. 187.

10. Rosenhead, L. (Ed.), Laminar Boundary Layers, (Oxford University Press, 1963).

11. Rouse, Hunter (Ed.), Advanced Mechanics of Fluids, (John Wiley & Sons, Inc., New York, 1959), p. 319.

12. Schlichting, Hermann, Boundary Layer Theory, 4th edition, (McGraw-Hill Book Company, New York, 1960).

13. Smith, A. M. O. and Clutter, Darwin W., "Solution of Prandtl's Boundary Layer Equations," Engineering Paper 1530, Douglas

Aircraft Company, Inc., Aircraft Division, Long Beach, California, February 1963.

14. Thwaites B., "Approximate Calculation of the Laminar Boundary Layer," The Aeronautical Quarterly, Vol. 1, November 1949, p. 245.